Research Square

Preprints are preliminary reports that have not undergone peer review.
They should not be considered conclusive, used to inform clinical practice,
or referenced by the media as validated information.

Diagnostic marker development for functional Lr21 and its validation in pyramiding with Pm36 in wheat

Yuqing Jin
Hebei Agricultural University
Yuanxia Liu
Hebei Agricultural University
Songsong Shen
Hebei Agricultural University
Shitao Yuan
Hebei Agricultural University
Changshan Liu
Hebei Agricultural University
Peiyuan Xu
Hebei Agricultural University
Chengyi Yan
Hebei Agricultural University
Haiyan Wang
wanghaiyan@hebau.edu.cn

Hebei Agricultural University

Research Article

Keywords: Wheat leaf rust, Lr21, Haplotype, Diagnostic marker, Pm36

Posted Date: September 14th, 2026

DOI: https://doi.org/10.21203/rs.3.rs-10746749/v1

License: This work is licensed under a Creative Commons Attribution 4.0 International License.
Read Full License

Additional Declarations: No competing interests reported.

Abstract

Background

The cloned avirulence gene AvrLr21 from *Puccinia triticina* (*Pt*) enables direct assessment of *Lr21* functionality via hypersensitive response (HR). Using this system, we evaluated 25 Chinese wheat cultivars that were previously identified as *Lr21*-positive by molecular markers.

Results

Unexpectedly, none of them exhibited HR upon AvrLr21 infiltration, indicating that all these accessions carry non-functional *Lr21* alleles. Sequence comparison further resolved these non-functional alleles into two distinct haplotypes: H1 (14 cultivars) and H2 (11 cultivars). Comparative sequencing revealed six polymorphic sites that distinguished functional from non-functional *Lr21* alleles, prompting development of a CAPS marker for functionality and four SSP markers for H1/H2 subtyping. Genotyping confirmed that all tested Chinese accessions carried only non-functional haplotypes, indicating no historical deployment of functional *Lr21*. As a proof of concept for marker utility, we pyramided functional *Lr21* with *Pm36* in a cross between TcLr21 and ZKPm36, obtaining F_2 progenies with the expected 29:9:9:3 segregation. Resistance assays of the pyramided plants revealed an expanded resistance spectrum (moderate leaf rust, high powdery mildew, moderate root rot) except against crown rot, defining the scope for deploying this dual-gene stack in breeding.

Conclusions

Collectively, we developed diagnostic markers discriminating functional from non-functional *Lr21* haplotypes, and validated their utility in pyramiding *Lr21* with *Pm36*, providing both tools and genetic materials for marker-assisted selection (MAS) and further improvement of multi-disease resistance in wheat.

Introduction

Wheat leaf rust, caused by the fungal pathogen *Puccinia triticina* (*Pt*), is a typical airborne fungal disease characterized by a wide dispersal range and high destructiveness. By impairing photosynthesis, the disease induces the depletion of nutrients in affected plants, thereby disrupting grain filling and typically causing yield losses of 5–10%, with severe infections leading to reductions of up to 50% [1]. The disease is globally distributed, with major epidemic regions including Canada, the United States and China [2]. Deployment of resistant cultivars remains the most effective strategy for managing wheat leaf rust. To date, over 100 leaf rust resistance genes have been identified on wheat chromosomes, among which *Lr85* is the most recently formally designated [3], and 13 genes have been cloned [3–5]. However, the high virulence variation of *Pt* frequently results in the breakdown of resistance. In China, genes such as

Lr9, *Lr19*, *Lr21*, *Lr24*, *Lr34*, *Lr38*, *Lr47*, and *Lr67* still confer effective resistance [6–8]. Therefore, continuous evaluation of the functional status of resistance genes in current cultivars is of critical importance for guiding rational cultivar deployment and ensuring durable disease control.

The wheat leaf rust resistance gene *Lr21* originated from *Aegilops tauschii* and was transferred into common wheat via distant hybridization in the 1970s, and was subsequently mapped to chromosome 1D [9]. Using a diploid/polyploid shuttle mapping strategy, Huang et al. successfully cloned *Lr21* through map-based cloning, and its encoded product was characterized as a typical NBS-LRR class disease resistance protein [10]. In natural populations, resistance genes often exhibit multiple haplotypes, which may differ in functional versus non-functional alleles. For example, the *RPM1* gene in *Arabidopsis thaliana* has two haplotypes that differ in their recognition of pathogen effectors [11]. Scherrer et al. found that the wheat leaf rust resistance gene *Lr10* also has two haplotypes: haplotype H1 carries both the intact *Lr10* gene and *RGA-2*, whereas haplotype H2 retains only a partial sequence of *RGA-2* [12]. With respect to *Lr21*, Huang et al. demonstrated that the wheat cultivars Wichita and Fielder each carry one haplotype on chromosome 1D, designated *Lr21-w* (H1) and *Lr21-f* (H2), respectively, both of which are non-functional alleles [13]. Corresponding haplotypes highly similar to *Lr21-w* and *Lr21-f* were also identified in the *Aegilops tauschii* population and named *Lr21-1* and *Lr21-2*, respectively. Naz et al. confirmed through population genomics analysis that *Lr21-w* and *Lr21-f* in common wheat originated from the introgression of *Lr21-1* and *Lr21-2* from *Aegilops tauschii* [14]. Given the functional differences among *Lr21* haplotypes in disease resistance, it is imperative to develop molecular markers that can effectively distinguish functional from non-functional haplotypes. Such markers would enable accurate assessment of the actual utilization of *Lr21* in Chinese wheat breeding programs, thereby providing a scientific basis for rational cultivar deployment and the improvement of durable disease resistance.

Wheat germplasm resources serve as the material foundation for wheat breeding. The exploration and utilization of elite leaf rust-resistant germplasm, as well as the development of multi-resistant wheat germplasm, are critical for safeguarding wheat production. Yang et al. constructed a multi-parental convergent crossing population, and after several generations of selection, obtained 168 F_6 lines [15]. Through molecular marker genotyping, field resistance evaluation, and agronomic trait assessment, they ultimately screened 19 lines with desirable agronomic traits, high resistance to stripe rust, and carrying the *Fhb1* gene. Zheng et al. pyramided the stripe rust resistance gene *Yr26*, the powdery mildew resistance gene ML91260, and the high-molecular-weight glutenin subunits Dx5 + Dy10 into a dwarf mutant of Xiaoyan 22, and successfully obtained six pyramided lines with combined resistance to stripe rust and powdery mildew, as well as superior quality [16]. Wang et al. developed a multiplex KASP (Multi-KASP) assay system that enables simultaneous detection of *Fhb7* and *Pm21*, which confer broad-spectrum resistance to *Fusarium* head blight and powdery mildew, respectively, and are derived from wild relatives of wheat [17]. Phenotypic evaluation demonstrated that pyramiding both genes enhanced resistance to both diseases. Multi-resistant wheat can effectively defend against infections by multiple pathogens, reduce yield losses caused by diseases, and improve yield stability, and has thus become an important direction for future wheat breeding.

Based on our previous screening of leading Chinese wheat cultivars (lines) using *Lr21*-specific molecular markers, we identified germplasm accessions carrying *Lr21* and validated their resistance to the prevalent wheat diseases, leaf rust and powdery mildew [18]. In the present study, we aim to further determine the functional type of *Lr21* through recognition with AvrLr21, identify haplotypes via sequence alignment, and develop diagnostic markers that distinguish functional from non-functional alleles. Subsequently, we will pyramid the functional *Lr21* allele with wheat materials that exhibit inferior leaf rust resistance but possess favorable resistance to other diseases, aiming to create novel multi-resistant germplasm. This study is designed to elucidate the functional status and haplotype distribution of *Lr21* in Chinese wheat, establish a precise identification system, and provide both genetic materials and a theoretical basis for multi-resistance breeding.

Results

Functional validation of Lr21 haplotypes through AvrLr21-triggered hypersensitive response

We previously cloned the avirulence gene *AvrLr21* from *Pt* and demonstrated that its gene product directly interacts with *Lr21* to trigger HR [19], and identified 25 germplasm accessions carrying *Lr21* using *Lr21*-specific molecular markers [18]. To further determine whether the *Lr21* alleles present in the 25 wheat cultivars (lines) carrying this gene correspond to functional haplotypes, we infiltrated purified AvrLr21 protein into the leaves of each of these 25 accessions. As shown in Fig. 1, none of the control treatments—GST protein, H_2O, or buffer—elicited HR in TcLr21 (positive control), Thatcher (negative control), or any of the 25 *Lr21*-carrying cultivars (lines). In contrast, the purified AvrLr21 protein induced a clear HR exclusively in TcLr21, but not in Thatcher or in any of the 25 accessions. These results indicate that the *Lr21* alleles in the 25 wheat cultivars (lines) fail to recognize the AvrLr21 protein, suggesting that these accessions most likely harbor non-functional *Lr21* haplotypes.

Sequence polymorphisms distinguishing functional and non-functional haplotypes

To determine whether the *Lr21* alleles present in the 25 wheat cultivars (lines) correspond to non-functional haplotypes, we performed PCR amplification using the markers Sta3 and D14-R [13]. Agarose gel electrophoresis revealed that all 25 cultivars (lines), as well as the positive control TcLr21, amplified a specific band of approximately 1,700 bp, whereas this band was absent in the negative control Thatcher (Fig. 2a). Sequencing of the PCR products confirmed that the expected *Lr21*-specific fragments were obtained. Sequence alignment using DNAMAN software revealed that the sequences of 14 cultivars (lines) were identical to the non-functional H1 haplotype (Fig. 2b), accounting for 56% of the tested lines. These 14 cultivars include Shijiazhuang 11, Jingdong 23, Zhongmai 175, Jingdong 11, Jingdong 20, Baofeng 104, Jingdong 22, Tang Y958, Jingdong 12, Jingdong 18, Jing 9428, Lunxuan 987, Luyuan 205, and Yaomai 16. The remaining 11 cultivars (lines), including Hongmai 15-1, Aifeng 8, Gaoyou 2018, Jimai 21, Tang Y959, Luyuan 502, Tang Y2, Heng 4399, Tang Y605, Jinan 17, and Jimai 4,

showed sequences consistent with the non-functional H2 haplotype (Fig. 2b), representing 44%. None of the 25 cultivars (lines) carried a functional *Lr21* allele.

To distinguish functional *Lr21* from its two non-functional haplotypes (H1 and H2), we aligned partial sequences of the three alleles using SnapGene. Sequence alignment revealed that H1 and H2 each contained a *BstE* II recognition site at positions 734 bp and 719 bp, respectively, which was absent in the functional *Lr21* sequence (Fig. 3a). After *BstE* II digestion, the functional *Lr21* fragment remained uncut as a single 1,700 bp band, whereas both non-functional fragments were cleaved into 1,000 bp and 700 bp bands (Fig. 3b), as confirmed by sequencing (Table S1). A CAPS marker was thus developed to discriminate functional from non-functional *Lr21* alleles. To validate this marker, we digested the corresponding fragments from the 25 *Lr21*-carrying wheat cultivars (lines) with *BstE* II. All 25 accessions produced the two diagnostic bands (1,000 bp and 700 bp) (Fig. 3c), indicating that they uniformly carried non-functional *Lr21* alleles. These results were verified by sequencing, confirming the utility of this CAPS marker for discriminating *Lr21* functionality in wheat germplasm.

To discriminate between the two non-functional *Lr21* haplotypes (H1 and H2), we aligned their partial sequences and identified five polymorphisms (two single nucleotide substitutions and three deletions), based on which we designed four sequence-specific primer (SSP) markers: SSP-H1-1, SSP-H1-2, SSP-H2-1, and SSP-H2-2 (Fig. 4a). Validation with known H1 and H2 templates showed that SSP-H1-1 and SSP-H1-2 specifically amplified 319 bp and 150 bp bands, respectively, only from H1 DNA, whereas SSP-H2-1 and SSP-H2-2 produced 621 bp and 682 bp bands exclusively from H2 DNA (Fig. 4b, c; Table S1). When applied to the 25 *Lr21*-carrying cultivars, 14 accessions (including Tang Y958, Luyuan 205, Zhongmai 175, Jingdong 22, Shijiazhuang 11, Jingdong 20, Jingdong 11, Baofeng 104, Lunxuan 987, Jingdong 18, Jingdong 12, Jing 9428, Yaomai 16, and Jingdong 23) yielded the H1-specific bands (Fig. S1a, b), while the remaining 11 accessions (Jimai 4, Tang Y2, Gaoyou 2018, Aifeng 8, Heng 4399, Luyuan 502, Tang Y605, Jimai 21, Jinan 17, Tang Y959, and Hongmai 15-1) showed the H2-specific bands (Fig. S1c, d). Together, these four SSP markers enable unambiguous discrimination between the non-functional H1 and H2 haplotypes in wheat germplasm.

Mendelian segregation validates marker utility in Lr21-Pm36 pyramiding population

To introduce functional *Lr21* into Chinese wheat background, we crossed TcLr21 (functional *Lr21* donor, highly resistant to leaf rust, moderately susceptible to powdery mildew and crown rot, and susceptible to root rot) with ZKPm36 (carrying *Pm36*, highly resistant to powdery mildew, moderately resistant to root rot, and highly susceptible to leaf rust) (Fig. 6a–d; Table S2). Two F_1 hybrids were obtained and confirmed to carry both functional *Lr21* (positive for *Lr21*-linked markers, uncut by *BstE* II, and positive for haplotype-specific primers) and *Pm36* (positive for the *Pm36*-linked marker) (Fig. 6e–g). From the self-pollinated F_1, 50 F_2 progenies were genotyped, yielding 29 plants carrying both genes, 9 carrying only *Lr21*, 9 carrying only *Pm36*, and 3 carrying neither, fitting a 9:3:3:1 segregation ratio ($\chi^2 = 0.0622$, $P > 0.05$) (Fig. S4a–e). Resistance evaluation of the F_2 progeny showed that they exhibited moderate resistance to leaf rust (IT = 2), high resistance to powdery mildew (no visible lesions), moderate

susceptibility to crown rot (rotting length < half of plant height), and moderate resistance to root rot (26–50% lesion coverage) (Fig. 6h-i; Table S2), indicating that pyramiding of *Lr21* and *Pm36* confers a broad-spectrum resistance profile while the F_2 population segregates as expected for two independently inherited genes.

Disease resistance genes in wheat often give rise to different haplotypes through single nucleotide polymorphisms, resulting in distinct functional consequences. Singh et al. reported six haplotypes of the leaf rust resistance gene *Lr9*, designated Hap-□ through Hap-□ [21]. Scherrer et al. found that *Lr10* has two haplotypes: H1 contains both the intact *Lr10* gene and *RGA-2*, while H2 retains only a partial *RGA-2* sequence [12]. For *Lr21*, two non-functional haplotypes, H1 and H2, have been identified [13]. However, the currently available markers Sta3 and D14-R can only detect the presence or absence of *Lr21*, but cannot distinguish functional from non-functional haplotypes, nor discriminate between the H1 and H2 haplotypes.

Given the sequence differences among haplotypes, various SNP-based genotyping methods have been developed. Traditional gel-based approaches include CAPS and allele-specific PCR (AS-PCR). For instance, Gonzalez-Cendales et al. developed the CAPS7774 marker targeting allelic variation in the tomato *I-7 Fusarium* wilt resistance gene [22]. After restriction digestion, resistant cultivars produced two bands of 612 bp and 196 bp, whereas susceptible cultivars showed a single uncut band of 808 bp, enabling accurate discrimination of resistant and susceptible genotypes. Guan et al. identified five haplotypes of the soybean salt-tolerance gene *GmSALT3*, developed two CAPS markers and three InDel markers, and genotyped 1,242 accessions to reveal the selection dynamics of salt-tolerant haplotypes in Chinese soybean breeding, providing a tool for molecular identification of salt tolerance in soybean [23]. In this study, based on the sequence differences among the functional *Lr21* haplotype and the two non-functional haplotypes, we developed one CAPS marker capable of distinguishing functional *Lr21* from non-functional haplotypes, and four specific markers (SSP-H1-1, SSP-H1-2, SSP-H2-1, and SSP-H2-2) that precisely discriminate between the non-functional H1 and H2 haplotypes. Collectively, these five molecular markers enable accurate identification of different *Lr21* haplotypes, significantly improving detection efficiency and accuracy. This study demonstrates that the development of functional markers has become an important direction for precision selection in disease resistance breeding.

Wheat leaf rust and powdery mildew often occur simultaneously in the field, resulting in substantial yield losses and quality deterioration. A single resistance gene is insufficient to cope with diverse pathogen races, and gene pyramiding has proven to be an effective strategy for enhancing the durability of disease resistance. Yang et al. constructed a multi-parental convergent crossing population using MAS to pyramid the major *Fusarium* head blight resistance gene *Fhb1* with the adult-plant stripe rust resistance genes *Yr18*, *Yr28*, and *Yr36*, obtaining 168 F_6 lines [15]. Among these, 19 lines with high stripe rust resistance, carrying *Fhb1*, and exhibiting excellent agronomic performance were selected, some of which can be directly used as breeding parents, providing core germplasm for durable and broad-spectrum wheat disease resistance breeding. Pan et al. introduced the powdery mildew resistance gene *Pm60* and

the stripe rust resistance gene *YrU1* from *Triticum urartu* into common wheat through distant hybridization combined with marker-assisted tracking, creating novel hexaploid wheat germplasm with combined resistance to powdery mildew and stripe rust, which can serve as intermediate materials for disease resistance breeding [24].

Conclusions

In this study, we systematically evaluated the functional status of the leaf rust resistance gene *Lr21* in Chinese wheat germplasm using the AvrLr21-triggered HR assay. Our results revealed that functional *Lr21* is universally absent in the tested Chinese wheat cultivars, all of which carry either the H1 or H2 non-functional haplotypes. Based on sequence polymorphisms between functional and non-functional alleles, we developed a CAPS marker for discriminating functional vs. non-functional *Lr21*, and four SSP markers for precise H1/H2 subtyping. These diagnostic markers provide efficient tools for tracking *Lr21* haplotypes in breeding programs. Furthermore, we successfully pyramided functional *Lr21* with the powdery mildew resistance gene *Pm36*, and the resulting F_2 progenies exhibited an expanded resistance spectrum against multiple pathogens, demonstrating the potential of this gene combination for multi-disease resistance breeding. Our findings not only clarify the deployment status of *Lr21* in Chinese wheat but also provide both molecular tools and genetic materials for future resistance improvement.

Materials and methods

Plant materials and fungal isolates

The wheat near-isogenic line TcLr21 (carrying *Lr21*) and its susceptible recurrent parent Thatcher, along with the fungal isolates *Bipolaris sorokiniana* (*Bs*), *Fusarium pseudograminearum* (*Fp*), and *Blumeria graminis* f. sp. *tritici* (*Bgt*), as well as the *Pt* race PHNT, were maintained at the Wheat Leaf Rust Laboratory of Hebei Agricultural University. The 25 wheat cultivars (lines) carrying the *Lr21* gene were provided by the Wheat Research Institute, Tangshan Academy of Agricultural Sciences. The wheat line ZKPm36 was kindly provided by Professor Zhiyong Liu from the Institute of Genetics and Developmental Biology, Chinese Academy of Sciences. Eight wheat mini-core germplasm accessions, including Fengkang 2, Youbao, Lovrin 10, Beijing 8, Yumai 49, Xiaoyan 6, Xinong 6028, and Lumai 1, were generously supplied by Professor Xiaodong Wang from the College of Plant Protection, Hebei Agricultural University.

Validation via infiltration of purified AvrLr21 protein

The purified GST and AvrLr21 proteins stored in the laboratory were adjusted to a concentration of 0.1 mg/mL. To verify the *Lr21* haplotypes in the tested wheat cultivars, the purified AvrLr21 protein, GST protein, H_2O, and buffer were separately infiltrated into leaves of TcLr21, Thatcher, and the 25 *Lr21*-

positive cultivars, with H_2O and buffer serving as negative controls. HR was scored at 48 h post-infiltration.

Sequence analysis of functional and non-functional Lr21 haplotypes

Genomic DNA of the 25 *Lr21*-carrying wheat accessions was extracted from young leaves using the CTAB method. To determine whether the *Lr21* alleles present in these accessions are functional or non-functional, the haplotype-specific primers Sta3 and D14-R (Table S1) were used for PCR amplification. The PCR products were resolved by 1.5% agarose gel electrophoresis, purified, and subsequently sequenced. Sequence alignment was performed using SnapGene and DNAMAN software to identify polymorphic sites between functional and non-functional haplotypes.

Development of a functional CAPS marker for the Lr21 gene

To identify restriction enzyme recognition sites specific to the functional *Lr21* allele and the two non-functional haplotypes (H1 and H2), the corresponding gene sequences were aligned using SnapGene software. Candidate restriction endonucleases were tested by single digestion of each haplotype, and the digestion products were resolved by 1.5% agarose gel electrophoresis to select the enzyme capable of discriminating the functional haplotype from the non-functional ones. The selected restriction enzyme was then used for single digestion of the amplified fragments from the 25 *Lr21*-carrying wheat accessions. All digestion products were confirmed by Sanger sequencing.

Detection of specific markers for the two non-functional Lr21 haplotypes

Based on the sequences of the non-functional H1 and H2 haplotypes obtained, sequence alignment was performed using DNAMAN software, and specific primers were designed based on the polymorphic sites between the two haplotypes (Table S1). PCR amplification was conducted using wheat DNA templates carrying either the H1 or H2 haplotype, and the primers that could stably and specifically amplify the expected bands were selected through agarose gel electrophoresis. The selected specific primers were then applied to PCR detection using DNA from the 25 *Lr21*-carrying wheat cultivars to determine whether these markers could effectively discriminate between the H1 and H2 haplotypes.

Haplotype analysis of Lr21 in wheat mini-core germplasm

To trace the origin and distribution of the *Lr21* gene, pedigrees of the *Lr21*-carrying wheat cultivars were established through literature review. Based on pedigree information and documented breeding records, eight wheat mini-core germplasm accessions carrying the *Lr21* gene were identified. Genomic DNA was extracted from young leaves using the CTAB method. The *Lr21* haplotypes in these mini-core accessions were then determined using the CAPS marker (for digestion-based detection) and the four SSP markers (for PCR-based genotyping) developed in this study. The results were resolved by 1.5% agarose gel electrophoresis.

Development and characterization of Lr21-Pm36 pyramiding population

To develop multi-resistant wheat germplasm pyramiding functional *Lr21* with *Pm36*, TcLr21 (as the male parent) was crossed with ZKPm36 (as the female parent) at the flowering stage to obtain F_1 seeds [25]. The F_1 plants were grown, and genomic DNA was extracted from leaf tissues. PCR detection was performed using molecular markers linked to *Lr21* and *Pm36*, together with the *Lr21* haplotype-specific markers developed in this study, to identify individual plants simultaneously carrying functional *Lr21* and *Pm36*. Self-pollinated seeds were harvested from the double-positive F_1 plants and sown to generate an F_2 population. The F_2 plants were subjected to the same genotyping assays

Disease resistance evaluation

Disease resistance evaluations were conducted in a greenhouse under controlled conditions. At the one-leaf-one-heart stage, plants were inoculated with *Pt*, *Bgt*, *Fp*, and *Bs*, respectively. For leaf rust and powdery mildew inoculations, plants were incubated in darkness at 22°C with high relative humidity for 14–18 h post-inoculation; for root rot inoculation, the incubation period was extended to 48 h. All inoculated plants were subsequently transferred to a greenhouse maintained at 25°C for routine cultivation. Infection types for leaf rust were recorded 14 days post-inoculation using the 0–4 scale described by Roelfs [26]. Powdery mildew resistance was evaluated following Ben-David et al. [27]. For crown rot, a grain-based inoculum was prepared and mixed with seeds at sowing, with a secondary inoculation performed at the one-leaf-one-heart stage; disease assessment followed Zhuang [28]. For root rot, a spore suspension (> 10^5 spores mL^{-1}) was sprayed onto seedlings, and resistance was evaluated according to Kokko et al. [29]. The susceptible controls were Thatcher (leaf rust), Mingxian 169 (powdery mildew), and Zhengzhou 5389 (crown rot and root rot). All experiments were performed with two independent replicates.All experiments were performed with at least three independent biological replicates, and representative results are shown in the figures.

Abbreviations

Pt
Puccinia triticina
AvrLr21
Avirulence gene corresponding to *Lr21*
Bgt
Blumeria graminis f. sp. *tritici*
Bs
Bipolaris sorokiniana
CAPS
Cleaved amplified polymorphic sequence
Fp
Fusarium pseudograminearum
HR

Hypersensitive response
MAS
Marker-assisted selection
NBS-LRR
Nucleotide-binding site leucine-rich repeat
Pm36
Powdery mildew resistance gene *Pm36*
SSP
Sequence-specific primer

Declarations

Ethics approval and consent to participate

Not applicable.

Consent for publication

Not applicable.

Competing interests

The authors declare no competing interests.

Funding

This study was funded by National Natural Science Foundation of China (32172384, 31501623) and Local Science, the Technology Development Fund Projects of Hebei Province Guided by the Central Government (246Z6504G), and the Hebei Province Dry Alkali Wheat Industry Technology System (HBCT2024030206).

Author Contribution

HW conceived and designed the experiments. YJ and YL performed the experiments, analyzed the data, and drafted the manuscript. SS, SY, and CL contributed to marker development, genotyping, and data analysis. PX and CY participated in field trials, disease resistance evaluation, and data collection. HW supervised the study and critically revised the manuscript. All authors read and approved the final manuscript.

Acknowledgement

We thank the Wheat Leaf Rust Laboratory of Hebei Agricultural University and the Wheat Research Institute of Tangshan Academy of Agricultural Sciences for their support. We are also grateful to Professor Zhiyong Liu from the Institute of Genetics and Developmental Biology, Chinese Academy of Sciences, and Professor Xiaodong Wang from the College of Plant Protection, Hebei Agricultural University, for providing valuable experimental materials.

Data Availability

All data generated or analysed during this study are included in this published article and its supplementary information files. The primer sequences used in this study are listed in Table S1.

References

1. Ordoñez ME, Germán SE, Kolmer JA. Genetic differentiation within the *Puccinia triticina* population in South America and comparison with the North American population suggests common ancestry and intercontinental migration. Phytopathology. 2010;100(4):376–83.
2. Liu T, Chen W. Race and virulence dynamics of *Puccinia triticina* in China during 2000–2006. Plant Dis. 2012;96(11):1601–7.
3. Sharon A, Sharma D, Avni R, Gutierrez-Gonzalez J, Kumar R, Sela H, Prusty M, Cohen A, Molnar I, Holuová K. A single NLR gene confers resistance to leaf and stripe rust in wheat. Nat Commun. 2024;15(1):9925.
4. Yang J, Li H, Li M, Song R, Shen T, Wang G, Xu D, Hao M, Jia A, Rehman SU, et al. Genome-assisted identification of wheat leaf rust resistance gene *Lr.ace-4A*/*Lr30*. Nat Commun. 2025;16(1):9339.
5. Yang G, Zhang N, Boshoff W, Li H, Li B, Zheng Q. Identification and introgression of a novel leaf rust resistance gene from *Thinopyrum intermedium* chromosome 7Js into wheat. Theor Appl Genet. 2023;136(11):231.
6. Zhang L, Zhao X, Liu J, Wang X, Gong W, Zhang Q, Liu Y, Yan H, Meng Q, Liu D. Evaluation of the resistance to Chinese predominant races of *Puccinia triticina* and analysis of effective leaf rust resistance genes in wheat accessions from the U.S. National Plant Germplasm System. Front Plant Sci. 2022;13:1054673.
7. Li H, Huang L, Zhang H, Liu B, Gao L, Chen W, Liu T. Race and virulence dynamics of *Puccinia triticina* in China during 2007 to 2021. Plant Dis. 2024;108(2):256–63.
8. Li H, Hua L, Zhao S, Hao M, Song R, Pang S, Liu Y, Chen H, Zhang W, Shen T, et al. Cloning of the wheat leaf rust resistance gene *Lr47* introgressed from *Aegilops speltoides*. Nat Commun. 2023;14(1):6072.
9. Rowland GG, Kerber ER. Telocentric mapping in hexaploid wheat of genes for LEAF rust resistance and other characters derived from *Aegilops squarrosa*. Can J Genet Cytol. 1974;16(1):137–44.

10. Huang L, Brooks SA, Li WL, Fellers JP, Trick HN, Gill BS. Map-based cloning of leaf rust resistance gene *Lr21* from the large and polyploid genome of bread wheat. Genetics. 2003;164(2):655–64.
11. Grant MR, Godiard L, Straube E, Ashfield T, Lewald J, Sattler A, Innes RW, Dangl JL. Structure of the *Arabidopsis RPM1* gene enabling dual-specificity disease resistance. Science. 1995;269(5225):843–6.
12. Scherrer B, Keller B, Feuillet C. Two haplotypes of resistance gene analogs have been conserved during evolution at the leaf rust resistance locus *Lr10* in wild and cultivated wheat. Funct Integr Genomics. 2002;2(1–2):40–50.
13. Huang L, Brooks SA, Li WL, Fellers J, Nelson JC, Gill B. Evolution of new disease specificity at a simple resistance locus in a crop-weed complex: reconstitution of the *Lr21* gene in wheat. Genetics. 2009;182(2):595–602.
14. Naz AA, Bungartz A, Serfling A, Kamruzzaman M, Schneider M, Wulff BBH, Pillen K, Ballvora A, Oerke EC, Ordon F, et al. *Lr21* diversity unveils footprints of wheat evolution and its new role in broad-spectrum leaf rust resistance. Plant Cell Environ. 2021;44(10):3445–58.
15. Yang X, Huang P, Yu B, Chen C, Gong H, Zhang Y, Huang K, Yang S, Hao M. Development of wheat lines pyramiding the *Fusarium* head blight resistance gene *Fhb1* with the stripe rust resistance genes *Yr18*, *Yr28*, and *Yr36*. Plants. 2026; 15(5):790.
16. Zheng W, Li S, Liu Z, Zhou Q, Feng Y, Chai S. Molecular marker assisted gene stacking for disease resistance and quality genes in the dwarf mutant of an elite common wheat cultivar Xiaoyan22. BMC Genet. 2020;21:45.
17. Wang Y, Yang J, Gao Y, Ma H, Dai Y, Ma H. Development and application of a cost-effective multiplex Kompetitive Allele-Specific PCR assay for pyramiding resistance genes of Fusarium head blight and powdery mildew in wheat. BMC Plant Biol. 2025;25:963.
18. Liu Y, Song M, Ding D, Jin Y, Liu C, Wang H, Wu Z. Detection of wheat leaf rust resistance gene *Lr21* and resistance evaluation to leaf rust and powdery mildew. Acta Agric Boreali-Sin. 2025;40(S1):240–7. (in Chinese).
19. Shen S, Wang F, Cui Z, Yuan S, Meng L, Liu D, Ma L, Wang H. *Puccinia triticina* avirulence protein AvrLr21 directly interacts with wheat resistance protein Lr21 to activate wheat immune response. Commun Biol. 2024;7:1170.
20. Zheng R. Molecular detection and gene postulation of leaf rust resistance gene in 262 Chinese wheat mini-core collections. Master's thesis. Yangling: Northwest A&F University; 2019. (in Chinese).
21. Singh J, Gudi S, Maughan PJ, Liu Z, Kolmer J, Wang M, Chen X, Rouse MN, Lasserre-Zuber P, Rimbert H, et al. Genomes of *Aegilops umbellulata* provide new insights into unique structural variations and genetic diversity in the U-genome for wheat improvement. Plant Biotechnol J. 2024;22:3505–19.
22. Gonzalez-Cendales Y, Catanzariti AM, Baker B, Mcgrath DJ, Jones DA. Identification of *I-7* expands the repertoire of genes for resistance to *Fusarium* wilt in tomato to three resistance gene classes. Mol Plant Pathol. 2016;17(3):448–63.

23. Guan R, Yu L, Liu X, Li M, Chang R, Gilliham M, Qiu L. Selection of the salt tolerance gene *GmSALT3* during six decades of soybean breeding in China. Front Plant Sci. 2021;12:794241.
24. Pan W, Yang J, Zhang B, Zhang J, Sun J, Yang Z, Liu N, Wei W, Zhang Q, Fahima T et al. Development of hexaploid wheat germplasm with resistance to both powdery mildew and stripe rust by introgression of *Pm60* and *YrU1* from *Triticum urartu*. Plants. 2026; 15(12): 1802.
25. Li M, Zhang H, Xiao H, Zhu K, Shi W, Zhang D, Wang Y, Yang L, Wu Q, Xie J, et al. A membrane associated tandem kinase from wild emmer wheat confers broad-spectrum resistance to powdery mildew. Nat Commun. 2024;15:3124.
26. Roelfs AP. Race specificity and methods of study. Cereal Rust. 1984;4(2):131–64.
27. Ben-David R, Dinoor A, Peleg Z, Fahima T. Reciprocal hosts' responses to powdery mildew isolates originating from domesticated wheats and their wild progenitor. Front. Plant Sci. 2018;9:75.
28. Zhuang X. Identification of resistance and gene analysis of main and new wheat varieties to *Fusarium* crown rot in Huang-Huai Wheat Region. Master's thesis. Zhengzhou: Henan Agricultural University; 2023. (in Chinese).
29. Kokko EG, Conner RL, Kozub GC, Lee B. Quantification by image analysis of subcrown internode discoloration in wheat caused by common root rot. Phytopathology. 1993;83(9):976–81.

Figures



Fig. 1 Phenotypes of 25 wheat varieties (lines) containing *Lr21* gene infiltrated with AvrLr21 purified protein**.** Representative leaves from three independent experiments are shown.

Figure 1

See image above for figure legend.



Fig. 1 Phenotypes of 25 wheat varieties (lines) containing *Lr21* gene infiltrated with AvrLr21 purified protein**.** Representative leaves from three independent experiments are shown.

Figure 1

See image above for figure legend.



Fig. 1 Phenotypes of 25 wheat varieties (lines) containing *Lr21* gene infiltrated with AvrLr21 purified protein**.** Representative leaves from three independent experiments are shown.

Figure 1

See image above for figure legend.



Fig. 1 Phenotypes of 25 wheat varieties (lines) containing *Lr21* gene infiltrated with AvrLr21 purified protein**.** Representative leaves from three independent experiments are shown.

Figure 1

See image above for figure legend.

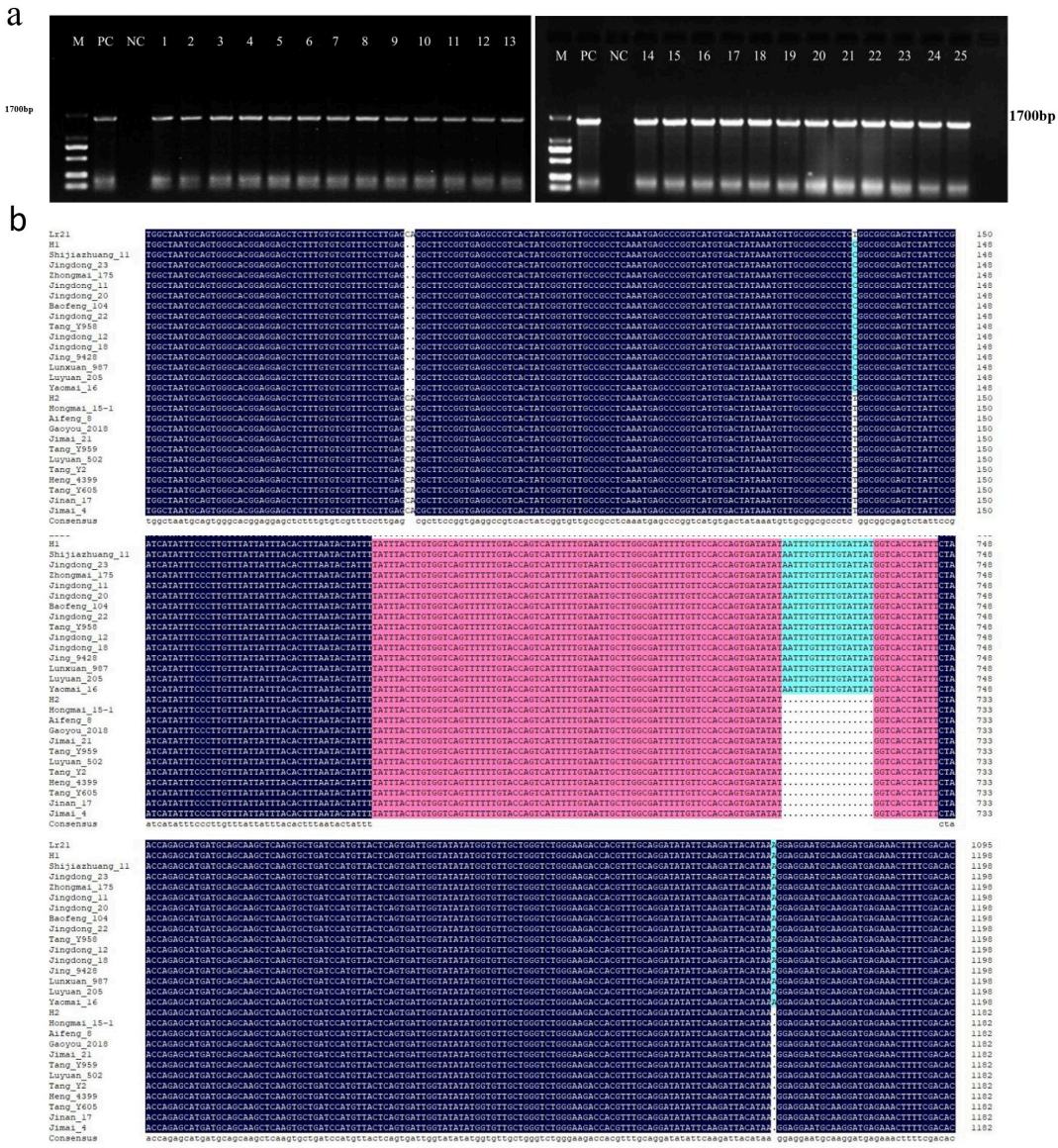


Fig. 2 Haplotype identification and sequence-based alignment of 25 wheat lines carrying the *Lr21* leaf rust resistance gene.

(a): PCR-based haplotype detection of *Lr21* using primers Sta3 and D14-R; M: DNA marker; PC: TcLr21; NC: Thatcher; 1: Tang Y958; 2: Jimai 4; 3: Tang Y2; 4: Luyuan 205; 5: Gaoyou 2018; 6: Zhongmai 175; 7: Jingdong 22; 8: Shijiazhuang 11; 9: Aifeng 8; 10: Jingdong 20; 11: Jingdong 11; 12: Heng 4399; 13: Baofeng 104; 14: Lunxuan 987; 15: Jingdong 18; 16: Jingdong 12; 17: Luyuan 502; 18: Jing 9428; 19: Tang Y605; 20: Jimai 21; 21: Jinan 17; 22: Yaomai 16; 23: Tang Y959; 24: Hongmai 15-1; 25: Jingdong 23. The expected amplicon is approximately 1,700 bp. **(b):** Partial sequence alignment showing H1 and H2 haplotypes. Representative results from three independent replicates are shown.

Figure 2

See image above for figure legend.

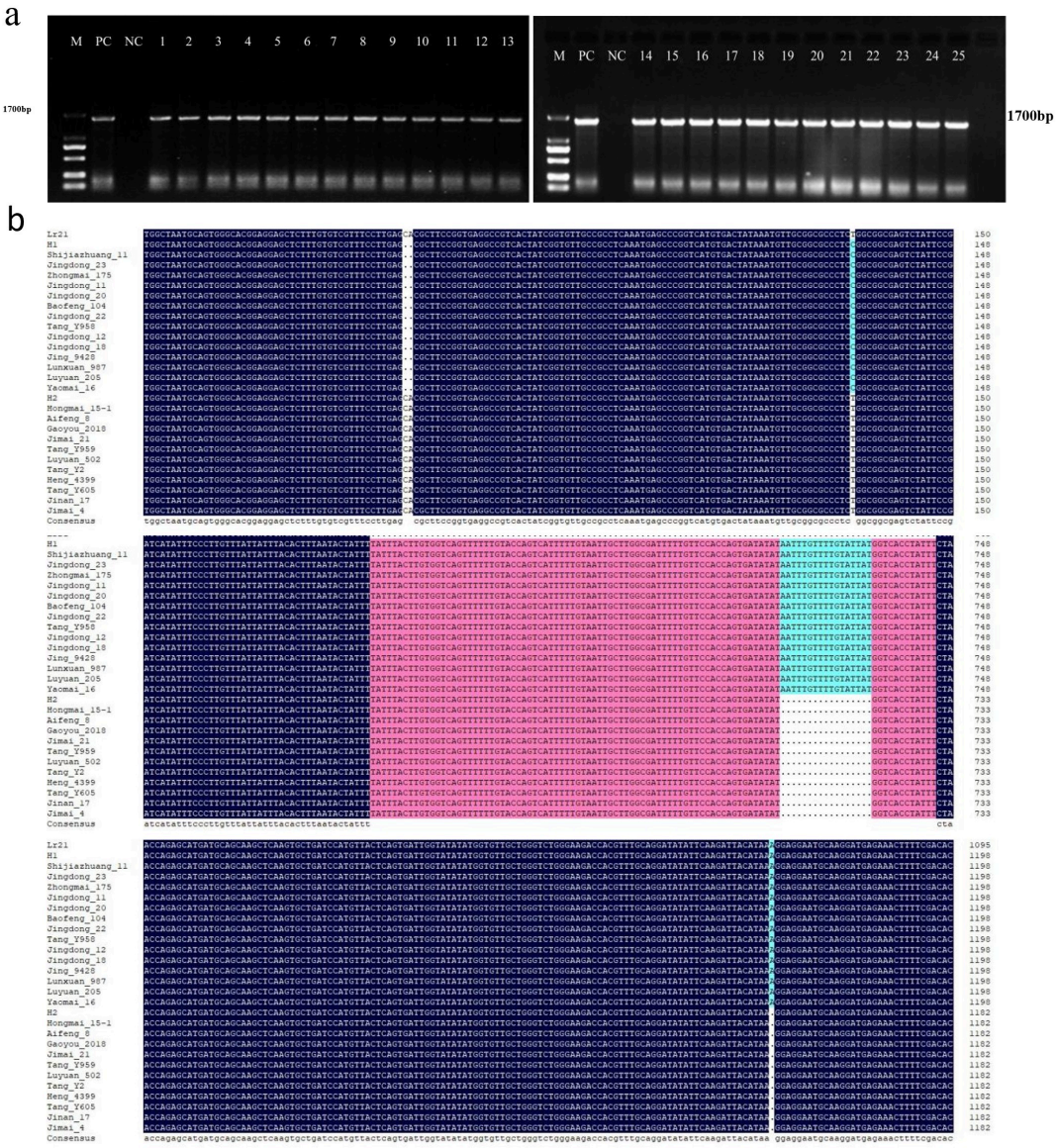


Fig. 2 Haplotype identification and sequence-based alignment of 25 wheat lines carrying the *Lr21* leaf rust resistance gene.

(a): PCR-based haplotype detection of *Lr21* using primers Sta3 and D14-R; M: DNA marker; PC: TcLr21; NC: Thatcher; 1: Tang Y958; 2: Jimai 4; 3: Tang Y2; 4: Luyuan 205; 5: Gaoyou 2018; 6: Zhongmai 175; 7: Jingdong 22; 8: Shijiazhuang 11; 9: Aifeng 8; 10: Jingdong 20; 11: Jingdong 11; 12: Heng 4399; 13: Baofeng 104; 14: Lunxuan 987; 15: Jingdong 18; 16: Jingdong 12; 17: Luyuan 502; 18: Jing 9428; 19: Tang Y605; 20: Jimai 21; 21: Jinan 17; 22: Yaomai 16; 23: Tang Y959; 24: Hongmai 15-1; 25: Jingdong 23. The expected amplicon is approximately 1,700 bp. **(b):** Partial sequence alignment showing H1 and H2 haplotypes. Representative results from three independent replicates are shown.

Figure 2

See image above for figure legend.

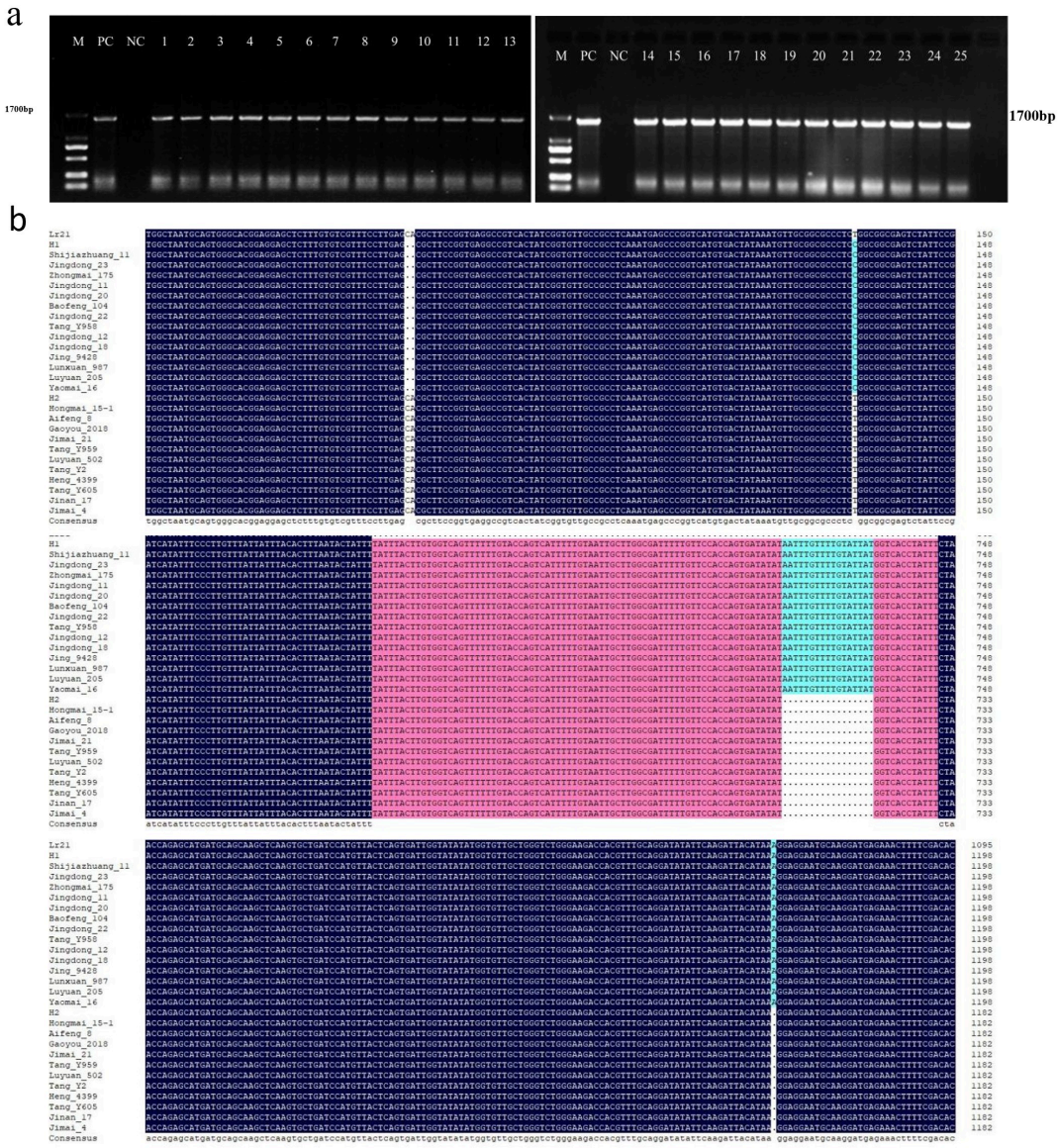


Fig. 2 Haplotype identification and sequence-based alignment of 25 wheat lines carrying the *Lr21* leaf rust resistance gene.

(a): PCR-based haplotype detection of *Lr21* using primers Sta3 and D14-R; M: DNA marker; PC: TcLr21; NC: Thatcher; 1: Tang Y958; 2: Jimai 4; 3: Tang Y2; 4: Luyuan 205; 5: Gaoyou 2018; 6: Zhongmai 175; 7: Jingdong 22; 8: Shijiazhuang 11; 9: Aifeng 8; 10: Jingdong 20; 11: Jingdong 11; 12: Heng 4399; 13: Baofeng 104; 14: Lunxuan 987; 15: Jingdong 18; 16: Jingdong 12; 17: Luyuan 502; 18: Jing 9428; 19: Tang Y605; 20: Jimai 21; 21: Jinan 17; 22: Yaomai 16; 23: Tang Y959; 24: Hongmai 15-1; 25: Jingdong 23. The expected amplicon is approximately 1,700 bp. **(b):** Partial sequence alignment showing H1 and H2 haplotypes. Representative results from three independent replicates are shown.

Figure 2

See image above for figure legend.

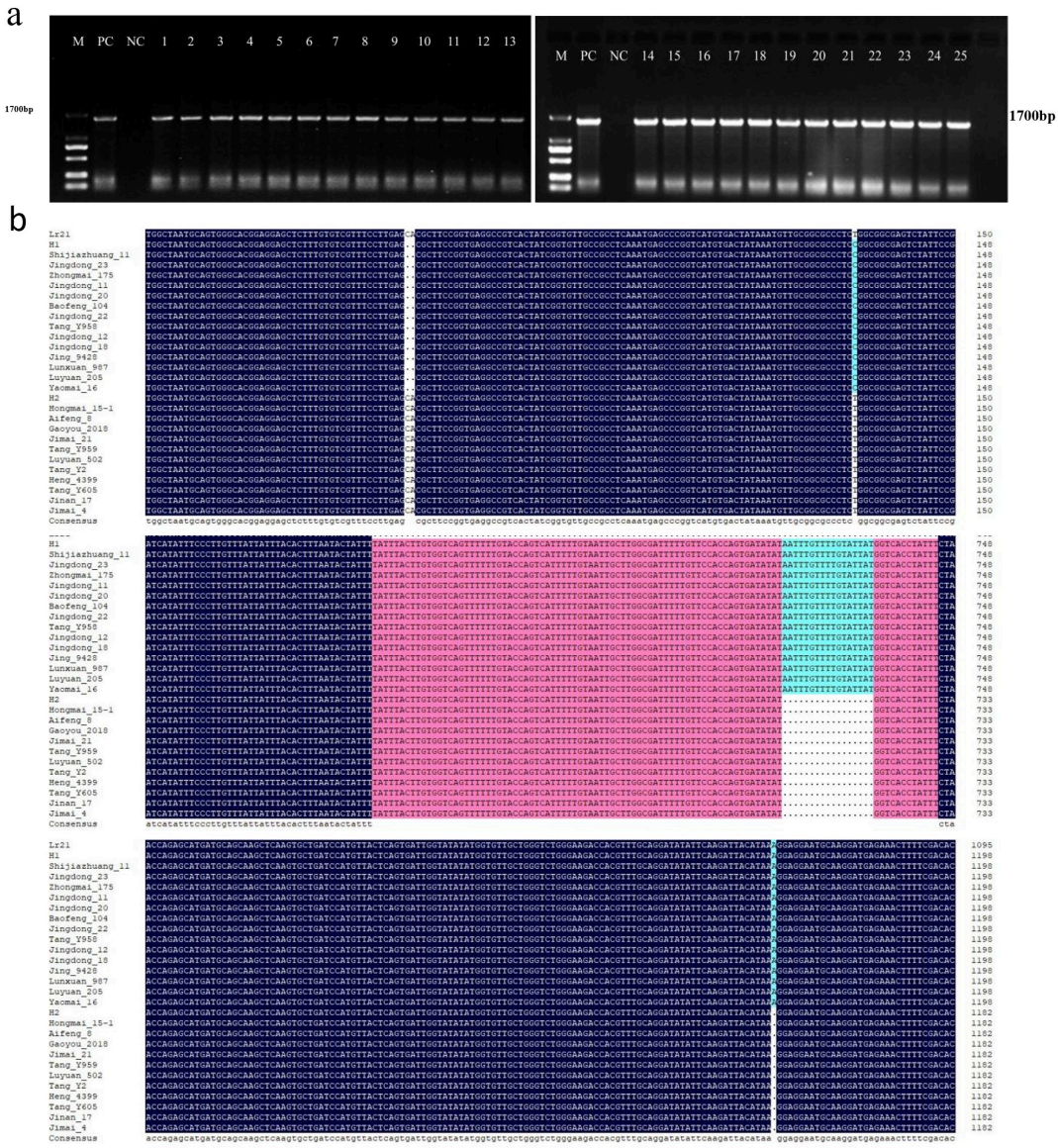


Fig. 2 Haplotype identification and sequence-based alignment of 25 wheat lines carrying the *Lr21* leaf rust resistance gene.

(a): PCR-based haplotype detection of *Lr21* using primers Sta3 and D14-R; M: DNA marker; PC: TcLr21; NC: Thatcher; 1: Tang Y958; 2: Jimai 4; 3: Tang Y2; 4: Luyuan 205; 5: Gaoyou 2018; 6: Zhongmai 175; 7: Jingdong 22; 8: Shijiazhuang 11; 9: Aifeng 8; 10: Jingdong 20; 11: Jingdong 11; 12: Heng 4399; 13: Baofeng 104; 14: Lunxuan 987; 15: Jingdong 18; 16: Jingdong 12; 17: Luyuan 502; 18: Jing 9428; 19: Tang Y605; 20: Jimai 21; 21: Jinan 17; 22: Yaomai 16; 23: Tang Y959; 24: Hongmai 15-1; 25: Jingdong 23. The expected amplicon is approximately 1,700 bp. **(b):** Partial sequence alignment showing H1 and H2 haplotypes. Representative results from three independent replicates are shown.

Figure 2

See image above for figure legend.

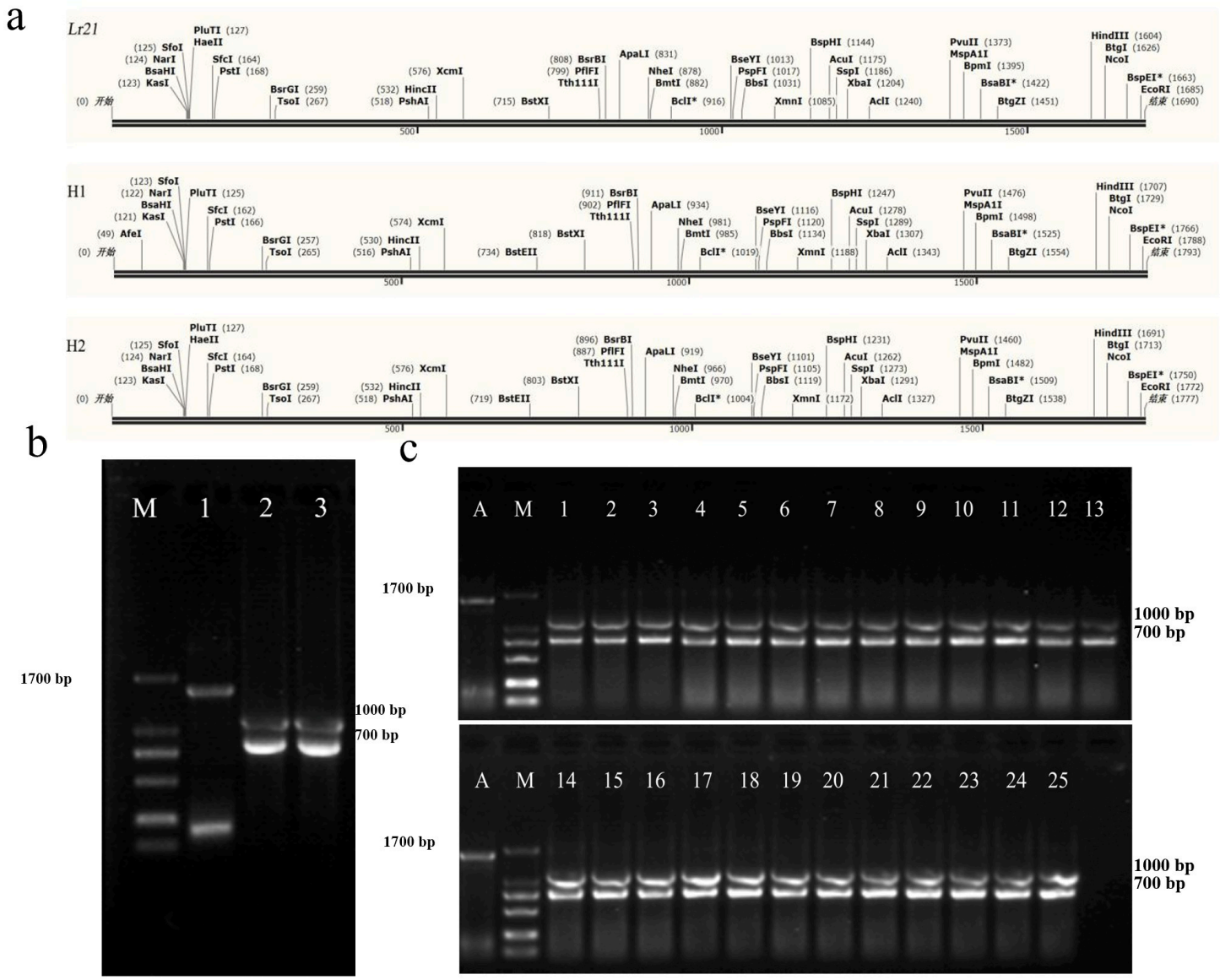


Fig. 3 Development and validation of a CAPS marker for the *Lr21* gene in wheat cultivars
(a): Partial sequence alignment of functional *Lr21*, H1 and H2 haplotypes showing the *BstE* II recognition sites in H1 (734 bp) and H2 (719 bp), which are absent in the functional sequence; **(b)**: *BstE* II digestion of functional *Lr21* (lane 1), H1 (lane 2), and H2 (lane 3). M: DNA marker; **(c)**: *BstE* II digestion of 25 *Lr21*-carrying wheat cultivars. A: TcLr21 (functional control); lanes 1–25: 25 cultivars. M: DNA marker. A representative result from three independent replicates is shown.

Figure 3

See image above for figure legend.

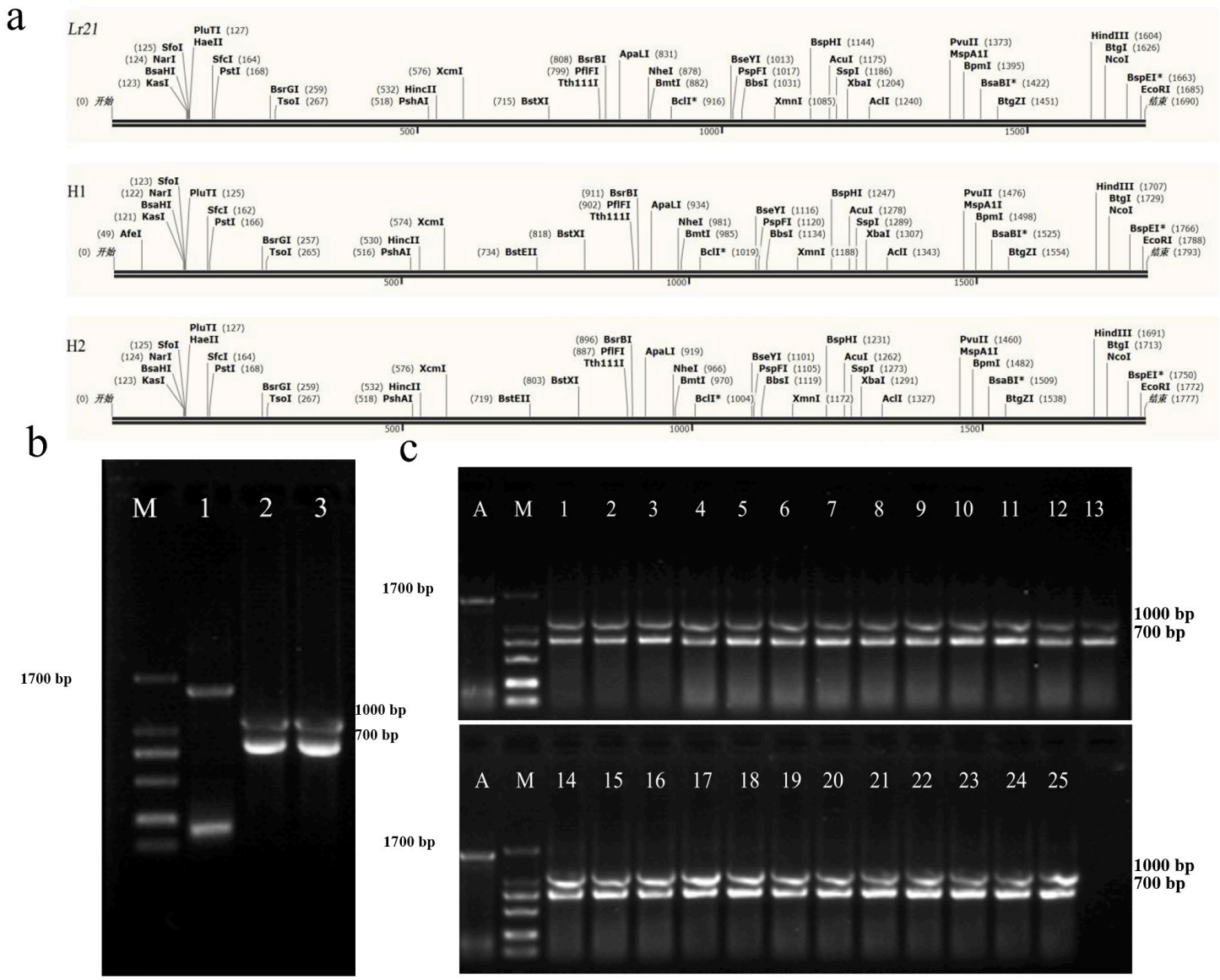


Fig. 3 Development and validation of a CAPS marker for the *Lr21* gene in wheat cultivars
(a): Partial sequence alignment of functional *Lr21*, H1 and H2 haplotypes showing the *BstE* II recognition sites in H1 (734 bp) and H2 (719 bp), which are absent in the functional sequence; **(b)**: *BstE* II digestion of functional *Lr21* (lane 1), H1 (lane 2), and H2 (lane 3). M: DNA marker; **(c)**: *BstE* II digestion of 25 *Lr21*-carrying wheat cultivars. A: TcLr21 (functional control); lanes 1–25: 25 cultivars. M: DNA marker. A representative result from three independent replicates is shown.

Figure 3

See image above for figure legend.

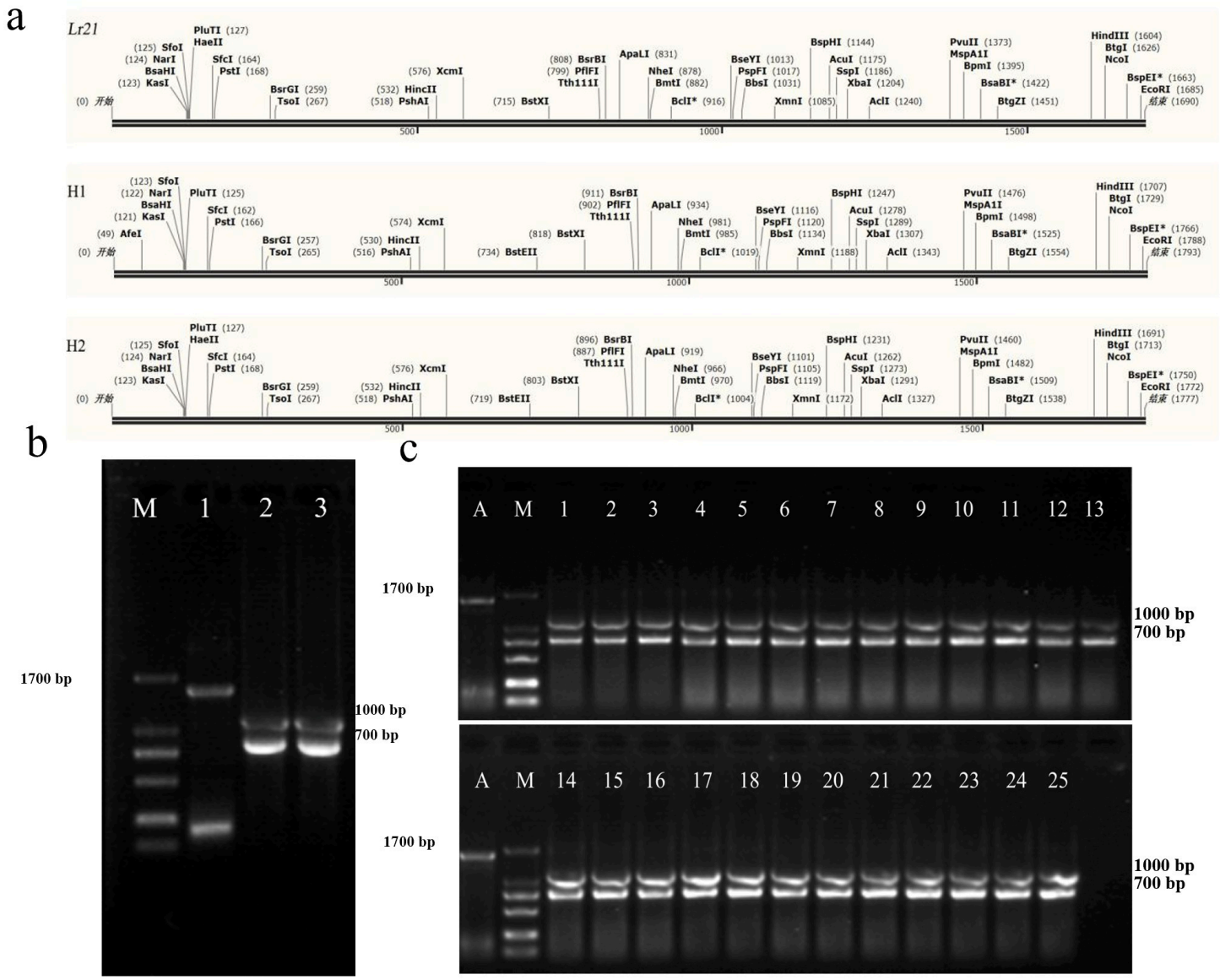


Fig. 3 Development and validation of a CAPS marker for the *Lr21* gene in wheat cultivars
(a): Partial sequence alignment of functional *Lr21*, H1 and H2 haplotypes showing the *BstE* II recognition sites in H1 (734 bp) and H2 (719 bp), which are absent in the functional sequence; **(b)**: *BstE* II digestion of functional *Lr21* (lane 1), H1 (lane 2), and H2 (lane 3). M: DNA marker; **(c)**: *BstE* II digestion of 25 *Lr21*-carrying wheat cultivars. A: TcLr21 (functional control); lanes 1–25: 25 cultivars. M: DNA marker. A representative result from three independent replicates is shown.

Figure 3

See image above for figure legend.

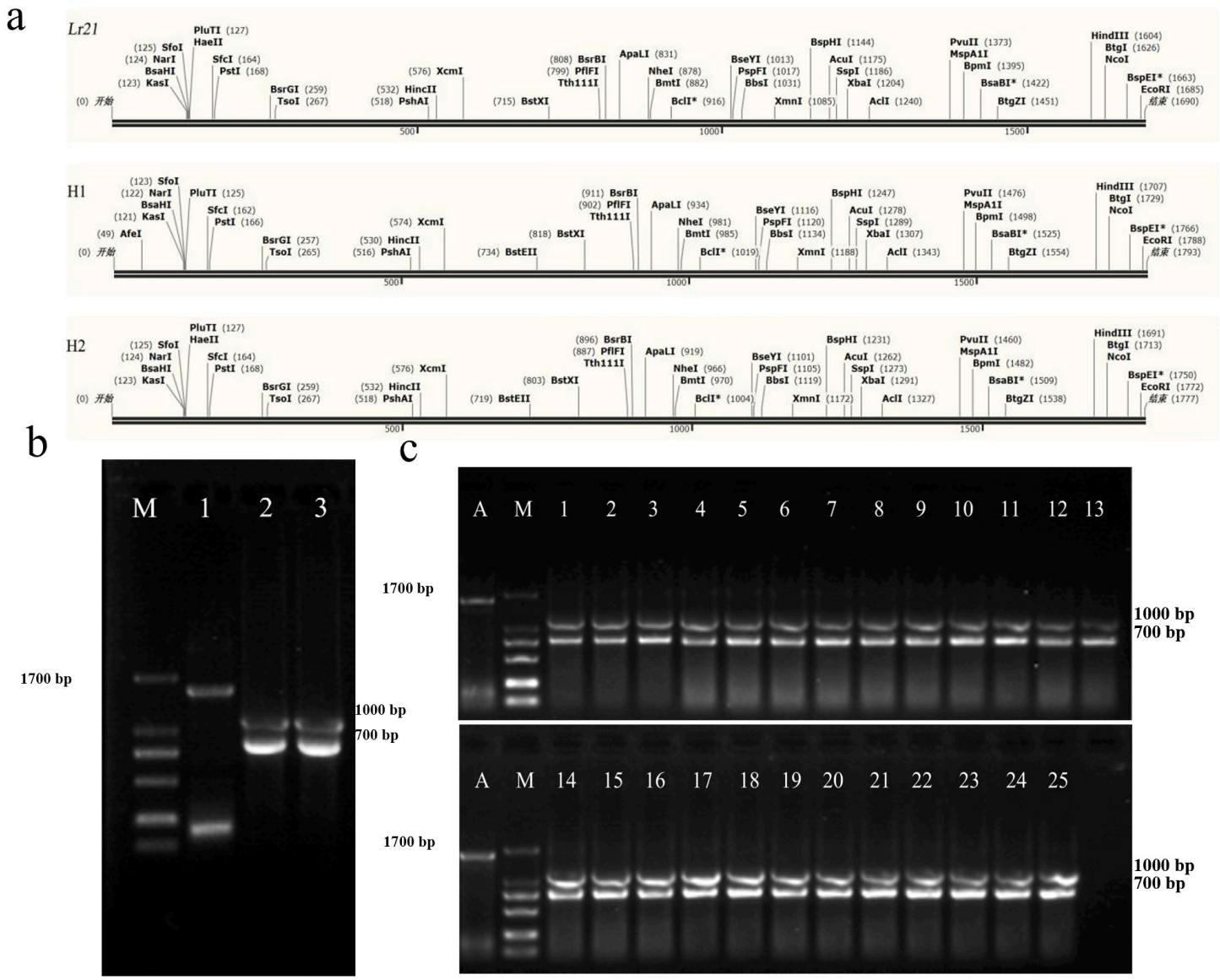


Fig. 3 Development and validation of a CAPS marker for the *Lr21* gene in wheat cultivars
(a): Partial sequence alignment of functional *Lr21*, H1 and H2 haplotypes showing the *BstE* II recognition sites in H1 (734 bp) and H2 (719 bp), which are absent in the functional sequence; **(b)**: *BstE* II digestion of functional *Lr21* (lane 1), H1 (lane 2), and H2 (lane 3). M: DNA marker; **(c)**: *BstE* II digestion of 25 *Lr21*-carrying wheat cultivars. A: TcLr21 (functional control); lanes 1–25: 25 cultivars. M: DNA marker. A representative result from three independent replicates is shown.

Figure 3

See image above for figure legend.

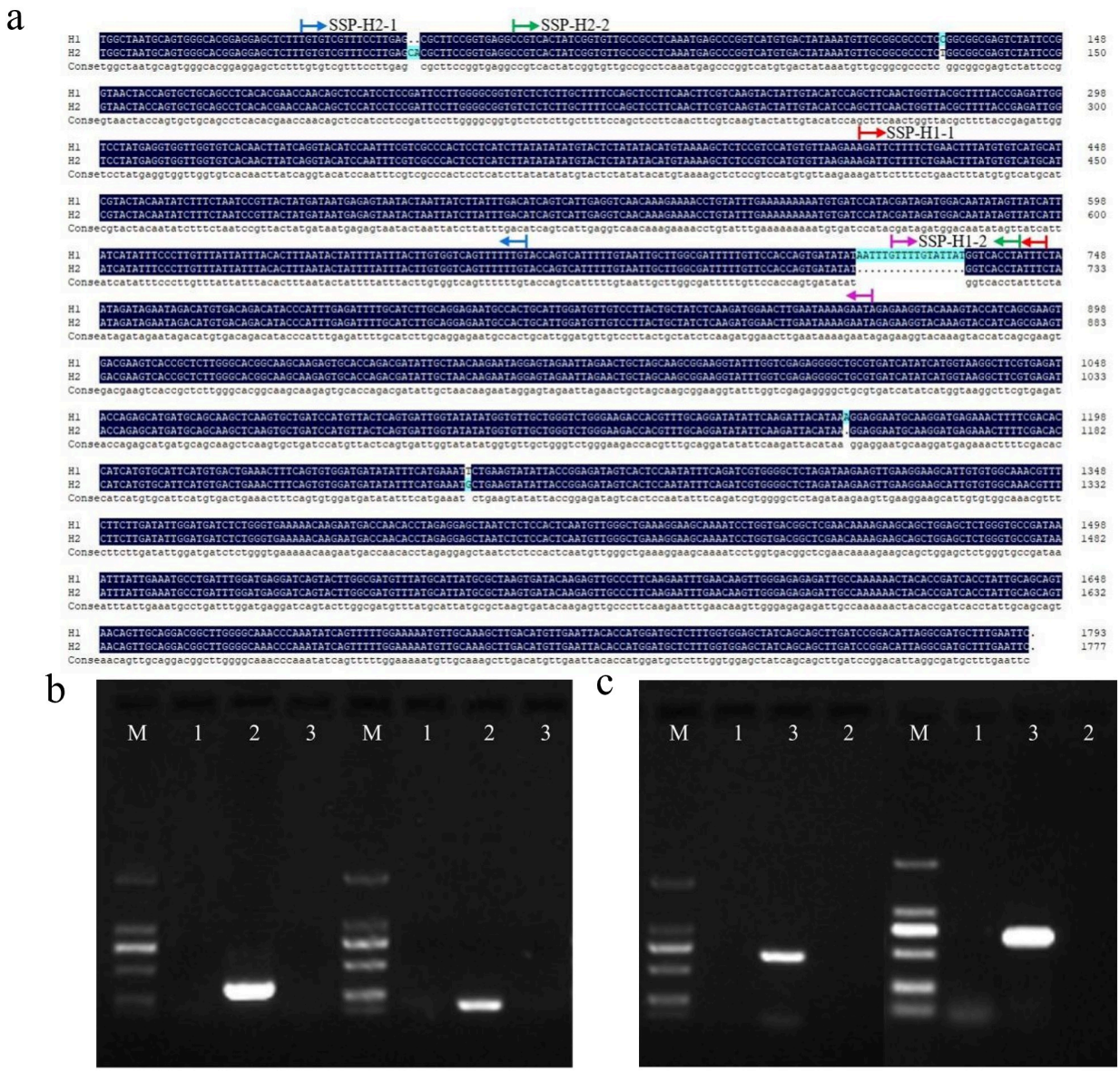


Fig. 4 Development of specific molecular markers of *Lr21* haplotypes

(a): Partial sequence alignment of H1 and H2 haplotypes showing five polymorphic sites (two single nucleotide substitutions and three deletions); **(b)**: Amplification results of SSP-H1-1 (319 bp) and SSP-H1-2 (150 bp) are specific to H1 DNA; **(c)**: Amplification results of SSP-H2-1 (621 bp) and SSP-H2-2 (682 bp) are specific to H2 DNA. M: DNA marker; 1: TcLr21; 2: H1 haplotype; 3: H2 haplotype. Representative results from three independent replicates are shown.

Figure 4

See image above for figure legend.

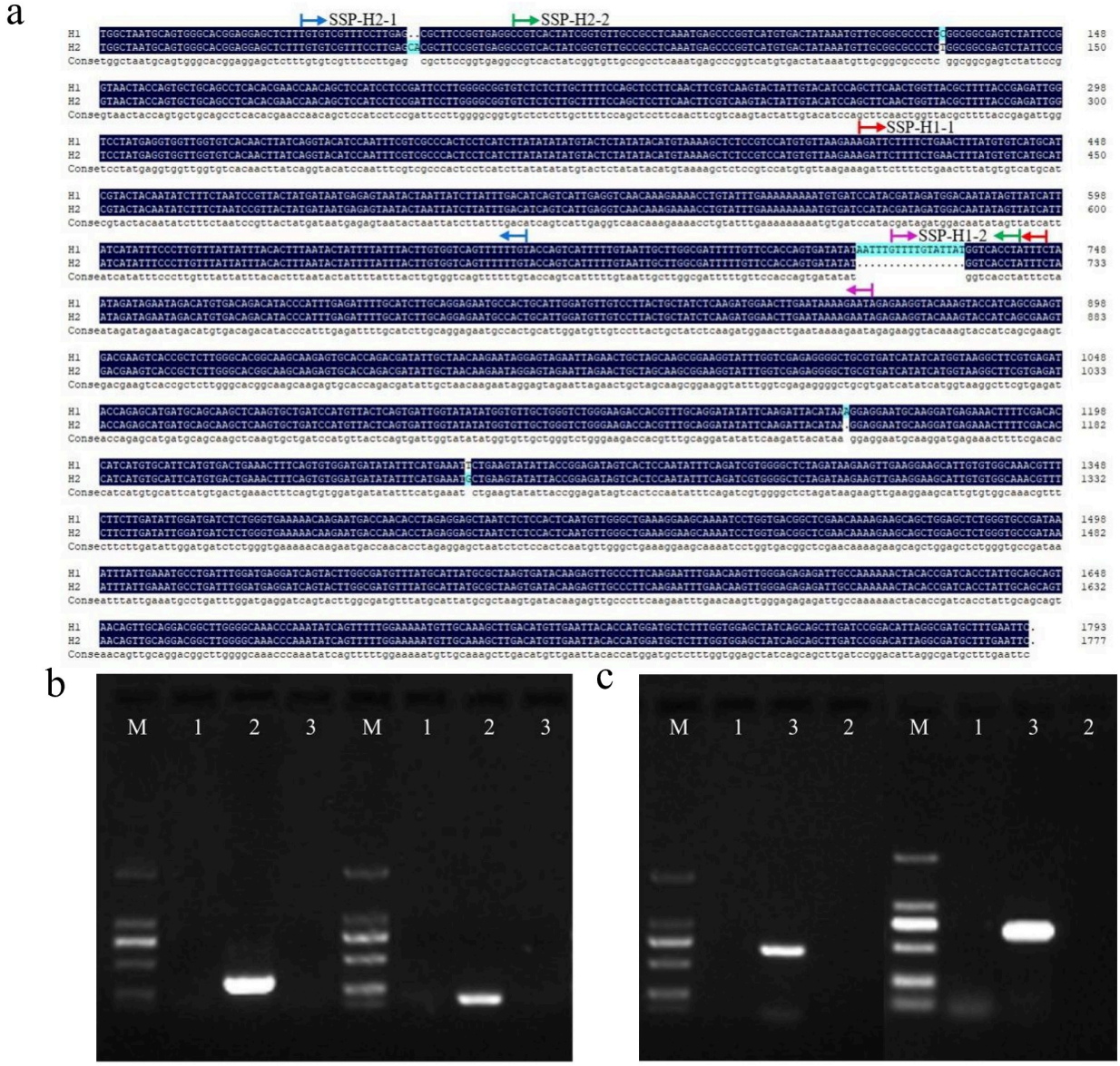


Fig. 4 Development of specific molecular markers of *Lr21* haplotypes

(a): Partial sequence alignment of H1 and H2 haplotypes showing five polymorphic sites (two single nucleotide substitutions and three deletions); **(b)**: Amplification results of SSP-H1-1 (319 bp) and SSP-H1-2 (150 bp) are specific to H1 DNA; **(c)**: Amplification results of SSP-H2-1 (621 bp) and SSP-H2-2 (682 bp) are specific to H2 DNA. M: DNA marker; 1: TcLr21; 2: H1 haplotype; 3: H2 haplotype. Representative results from three independent replicates are shown.

Figure 4

See image above for figure legend.

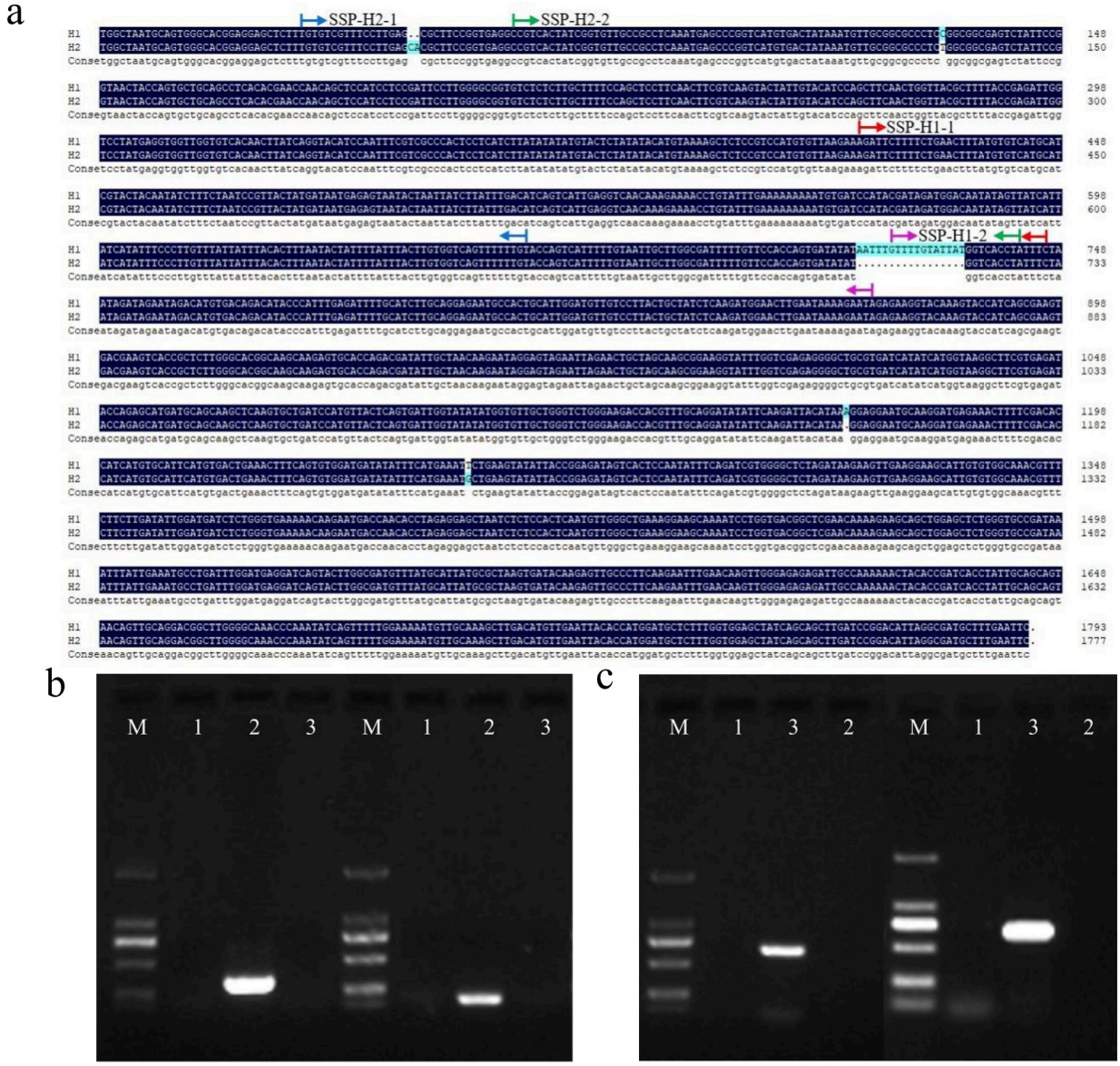


Fig. 4 Development of specific molecular markers of *Lr21* haplotypes

(a): Partial sequence alignment of H1 and H2 haplotypes showing five polymorphic sites (two single nucleotide substitutions and three deletions); **(b)**: Amplification results of SSP-H1-1 (319 bp) and SSP-H1-2 (150 bp) are specific to H1 DNA; **(c)**: Amplification results of SSP-H2-1 (621 bp) and SSP-H2-2 (682 bp) are specific to H2 DNA. M: DNA marker; 1: TcLr21; 2: H1 haplotype; 3: H2 haplotype. Representative results from three independent replicates are shown.

Figure 4

See image above for figure legend.

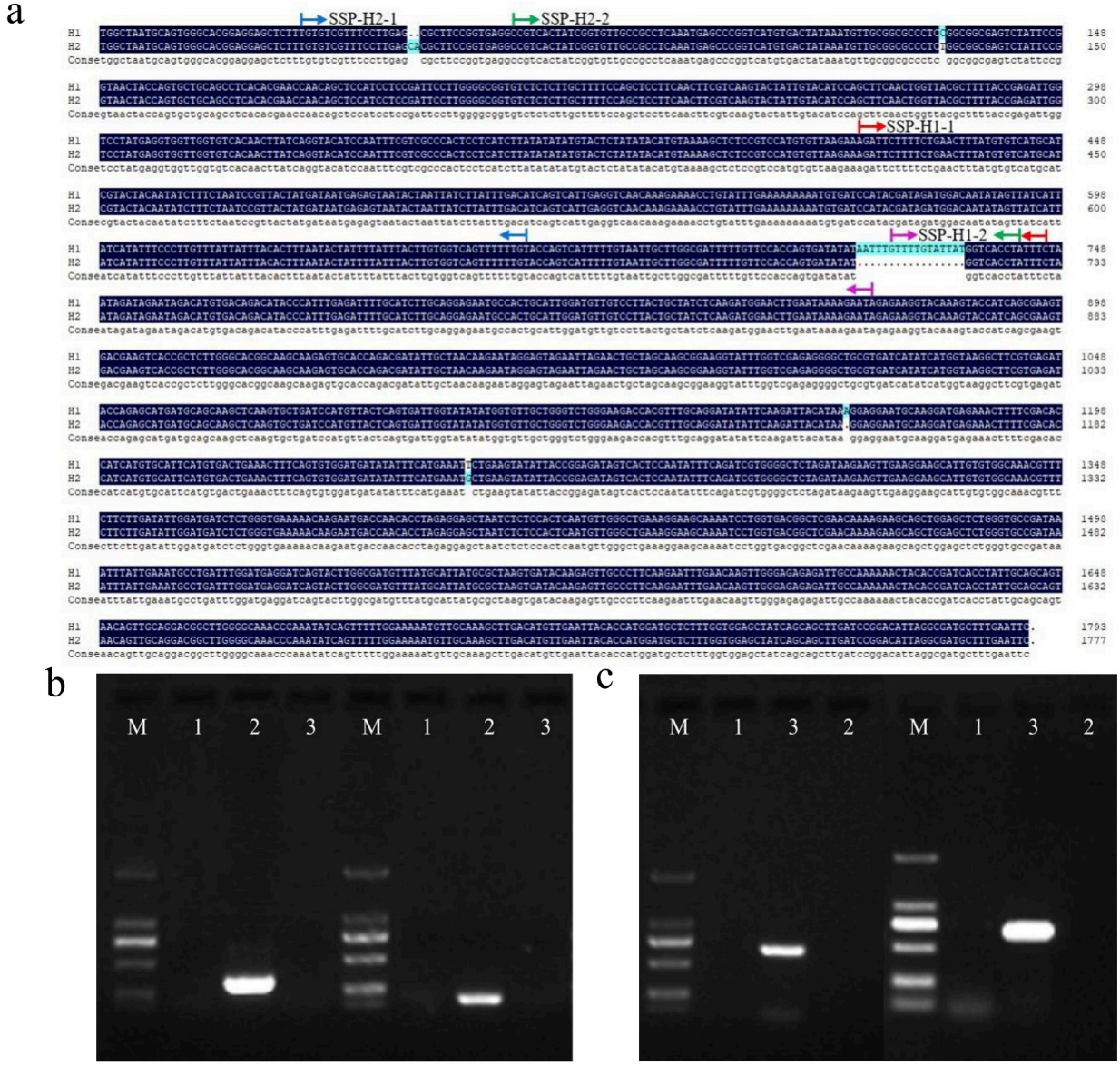


Fig. 4 Development of specific molecular markers of *Lr21* haplotypes

(a): Partial sequence alignment of H1 and H2 haplotypes showing five polymorphic sites (two single nucleotide substitutions and three deletions); **(b)**: Amplification results of SSP-H1-1 (319 bp) and SSP-H1-2 (150 bp) are specific to H1 DNA; **(c)**: Amplification results of SSP-H2-1 (621 bp) and SSP-H2-2 (682 bp) are specific to H2 DNA. M: DNA marker; 1: TcLr21; 2: H1 haplotype; 3: H2 haplotype. Representative results from three independent replicates are shown.

Figure 4

See image above for figure legend.

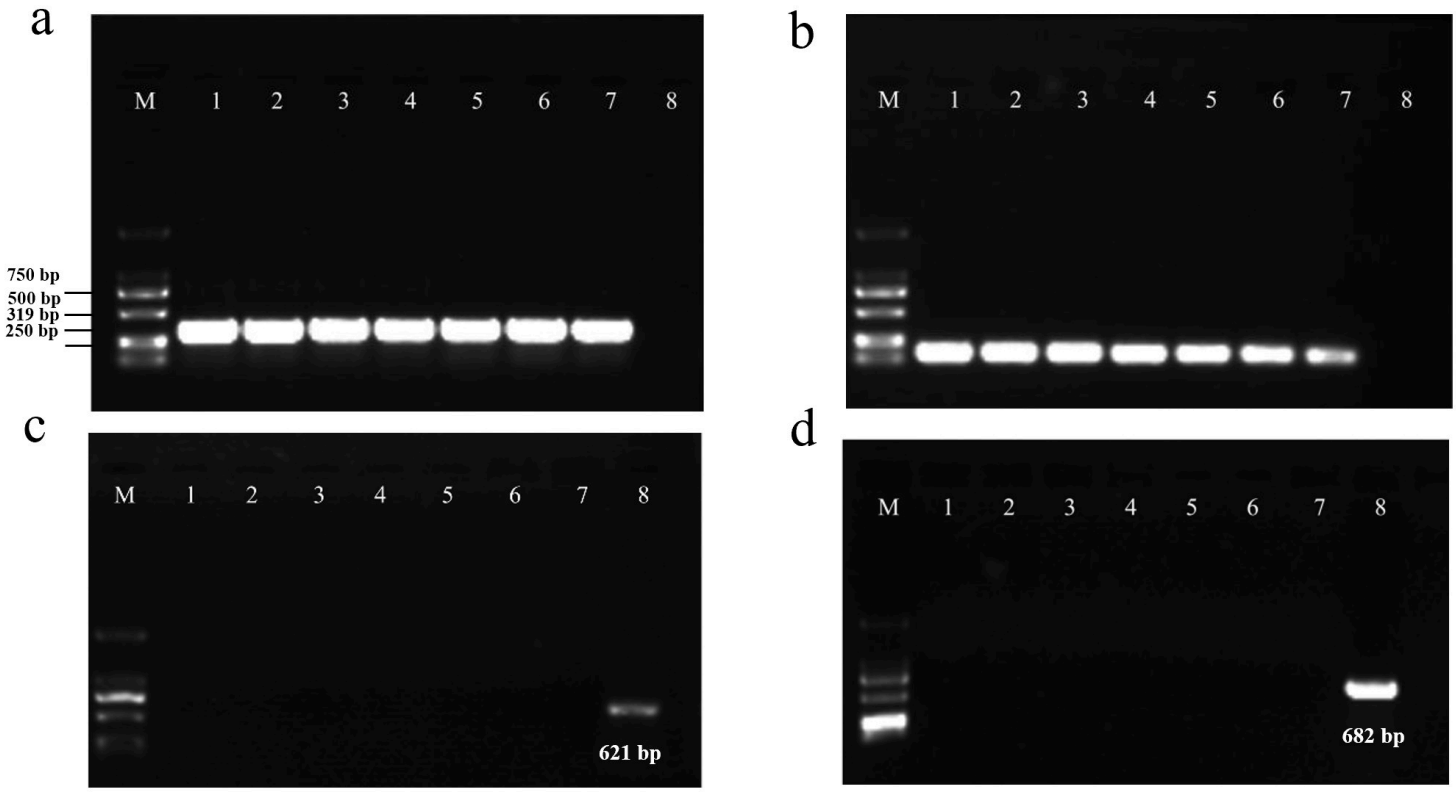


Fig. 5 Haplotype identification of eight wheat mini-core germplasm accessions using four SSP markers

(a): Amplification results of SSP-H1-1; **(b)**: SSP-H1-2; **(c)**: SSP-H2-1; **(d)**: SSP-H2-2. M: DNA marker; 1: Fengkang 2; 2: Youbao; 3: Lovrin 10; 4: Beijing 8; 5: Xiaoyan 6; 6: Xinong 6028; 7: Lumai 1; 8: Yumai 49. Accessions 1-7 amplified the H1-specific bands, whereas Yumai 49 (lane 8) amplified the H2-specific bands. Representative results from three independent replicates are shown.

Figure 5

See image above for figure legend.

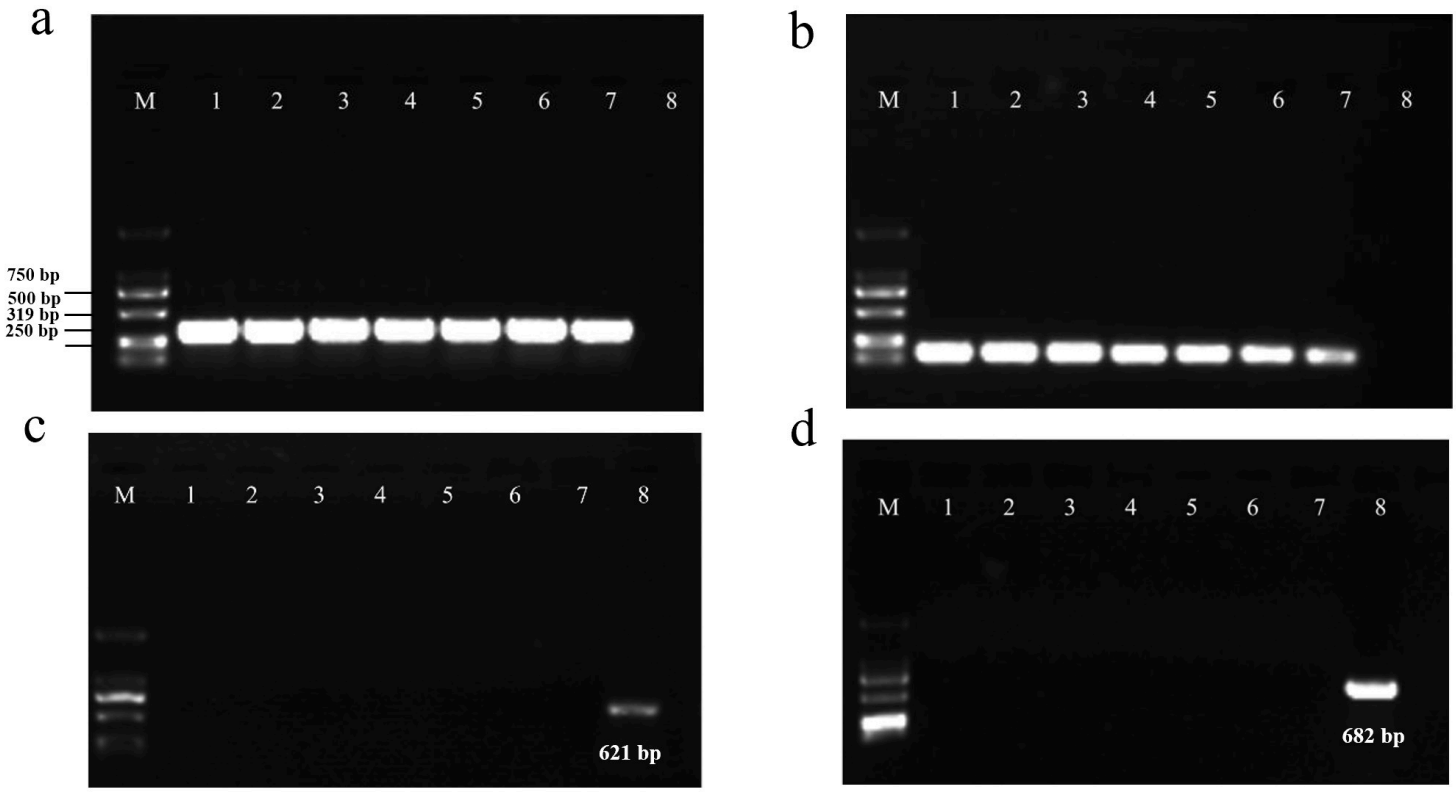


Fig. 5 Haplotype identification of eight wheat mini-core germplasm accessions using four SSP markers

(a): Amplification results of SSP-H1-1; **(b)**: SSP-H1-2; **(c)**: SSP-H2-1; **(d)**: SSP-H2-2. M: DNA marker; 1: Fengkang 2; 2: Youbao; 3: Lovrin 10; 4: Beijing 8; 5: Xiaoyan 6; 6: Xinong 6028; 7: Lumai 1; 8: Yumai 49. Accessions 1-7 amplified the H1-specific bands, whereas Yumai 49 (lane 8) amplified the H2-specific bands. Representative results from three independent replicates are shown.

Figure 5

See image above for figure legend.

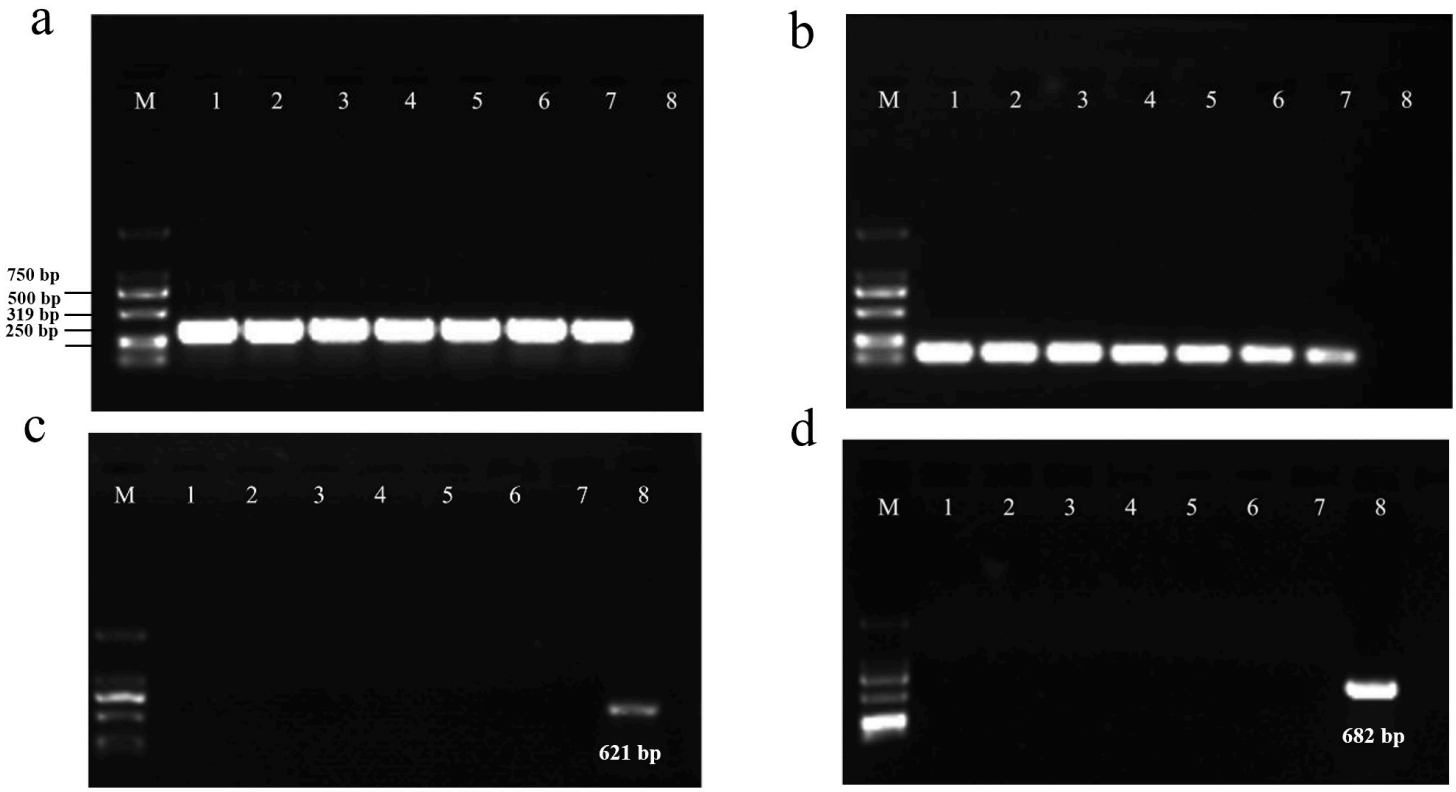


Fig. 5 Haplotype identification of eight wheat mini-core germplasm accessions using four SSP markers

(a): Amplification results of SSP-H1-1; **(b)**: SSP-H1-2; **(c)**: SSP-H2-1; **(d)**: SSP-H2-2. M: DNA marker; 1: Fengkang 2; 2: Youbao; 3: Lovrin 10; 4: Beijing 8; 5: Xiaoyan 6; 6: Xinong 6028; 7: Lumai 1; 8: Yumai 49. Accessions 1-7 amplified the H1-specific bands, whereas Yumai 49 (lane 8) amplified the H2-specific bands. Representative results from three independent replicates are shown.

Figure 5

See image above for figure legend.

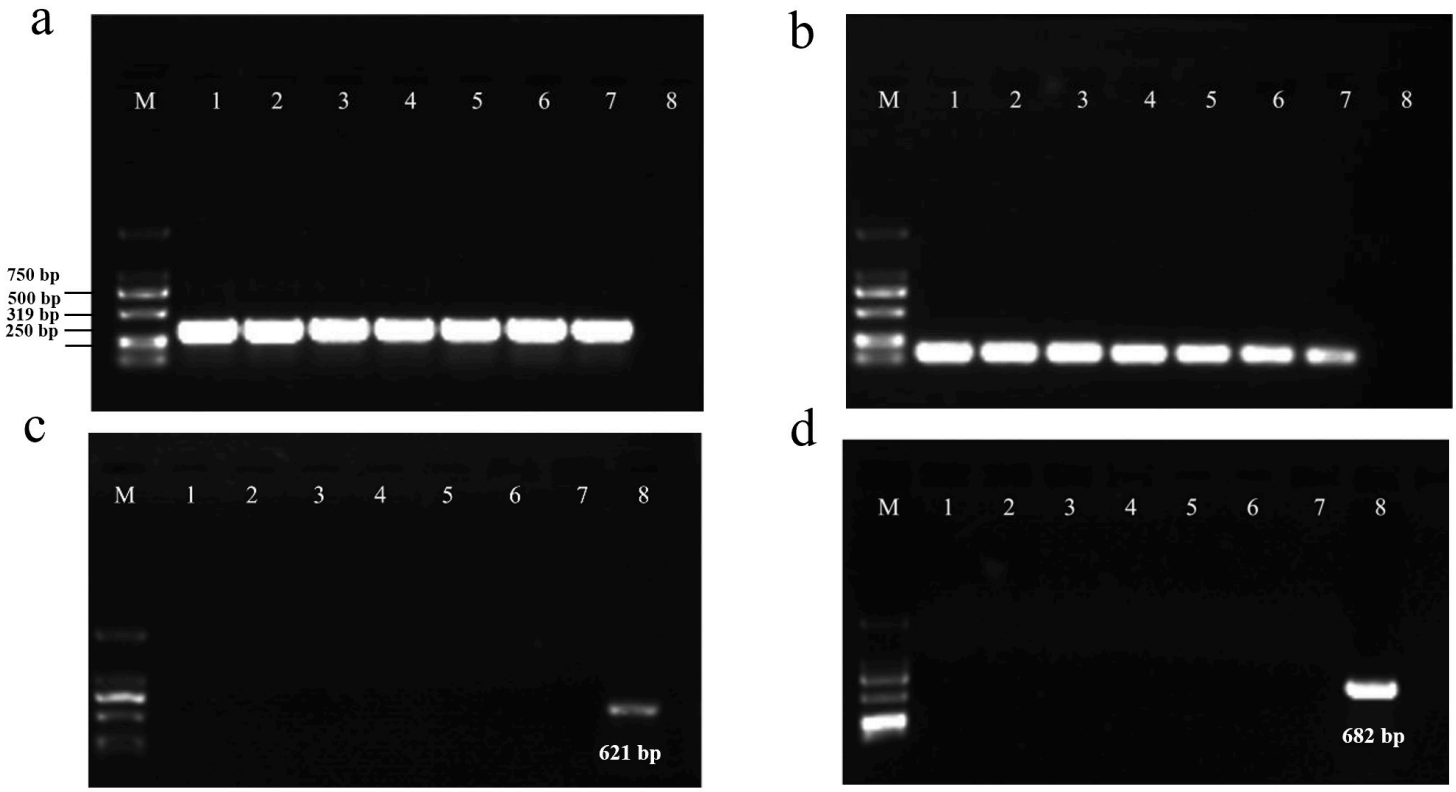


Fig. 5 Haplotype identification of eight wheat mini-core germplasm accessions using four SSP markers

(a): Amplification results of SSP-H1-1; **(b)**: SSP-H1-2; **(c)**: SSP-H2-1; **(d)**: SSP-H2-2. M: DNA marker; 1: Fengkang 2; 2: Youbao; 3: Lovrin 10; 4: Beijing 8; 5: Xiaoyan 6; 6: Xinong 6028; 7: Lumai 1; 8: Yumai 49. Accessions 1-7 amplified the H1-specific bands, whereas Yumai 49 (lane 8) amplified the H2-specific bands. Representative results from three independent replicates are shown.

Figure 5

See image above for figure legend.

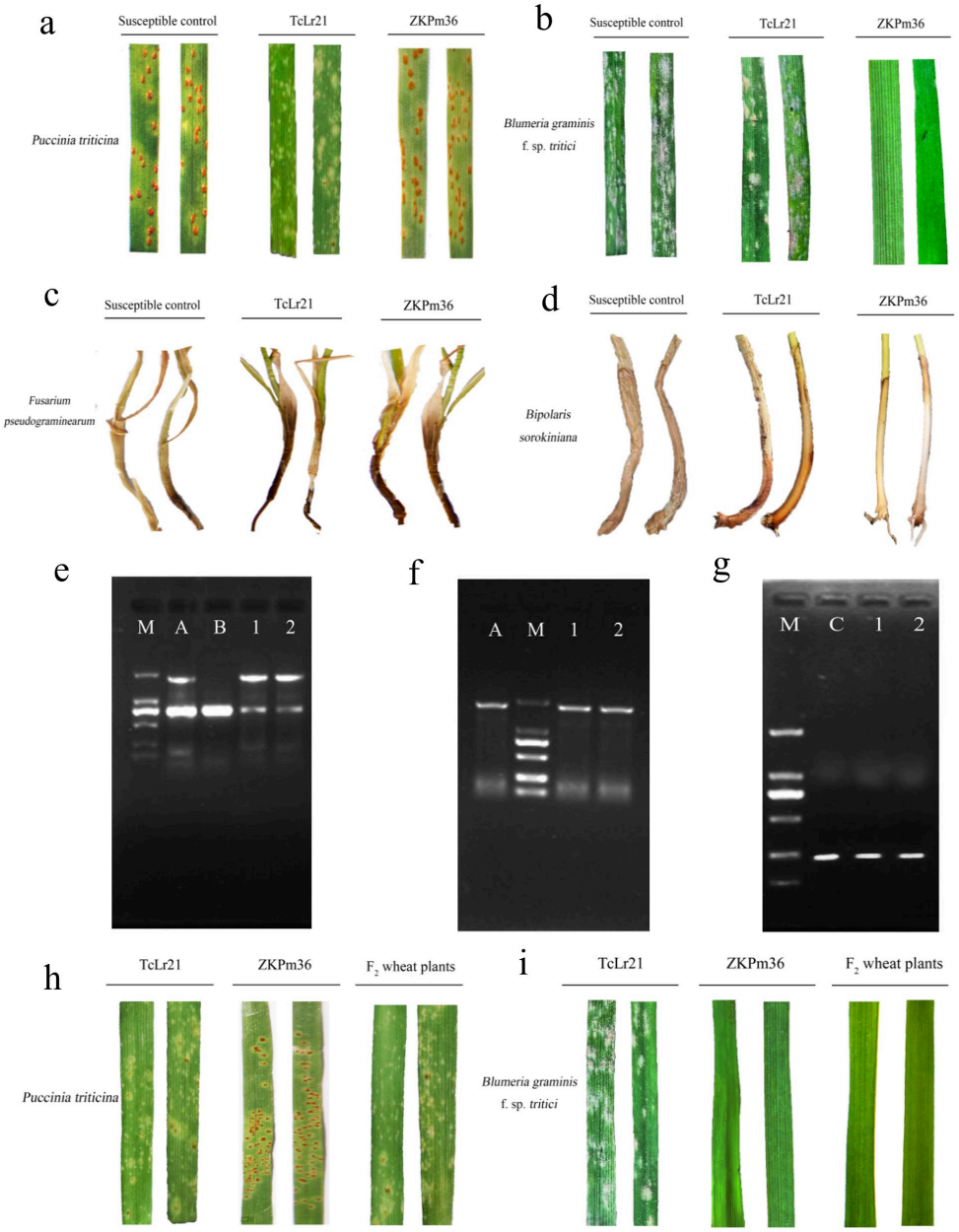


Fig. 6 Multi-disease resistance phenotyping and validation of parental lines TcLr21 and ZKPm36, their two hybrid progenies, and the F_2 generation

(a): Resistance to *Puccinia triticina* (leaf rust); **(b)**: *Blumeria graminis* f. sp. *tritici* (powdery mildew); **(c)**: *Fusarium pseudograminearum* (crown rot); **(d)**: *Bipolaris sorokiniana* (root rot) in TcLr21, Thatcher, and ZKPm36. **(e)**: Molecular detection of *Lr21*; **(f)**: *BstE* II digestion; **(g)**: Molecular detection of *Pm36* in F_1 hybrids. M: DNA marker; A: TcLr21; B: Thatcher; C: ZKPm36; 1-2: F_1 hybrids. **(h)** *Puccinia triticina* and **(i)** *Blumeria graminis* f. sp. *tritici*resistance in F_2 progenies. Representative results from three independent replicates are shown.

Figure 6

See image above for figure legend.

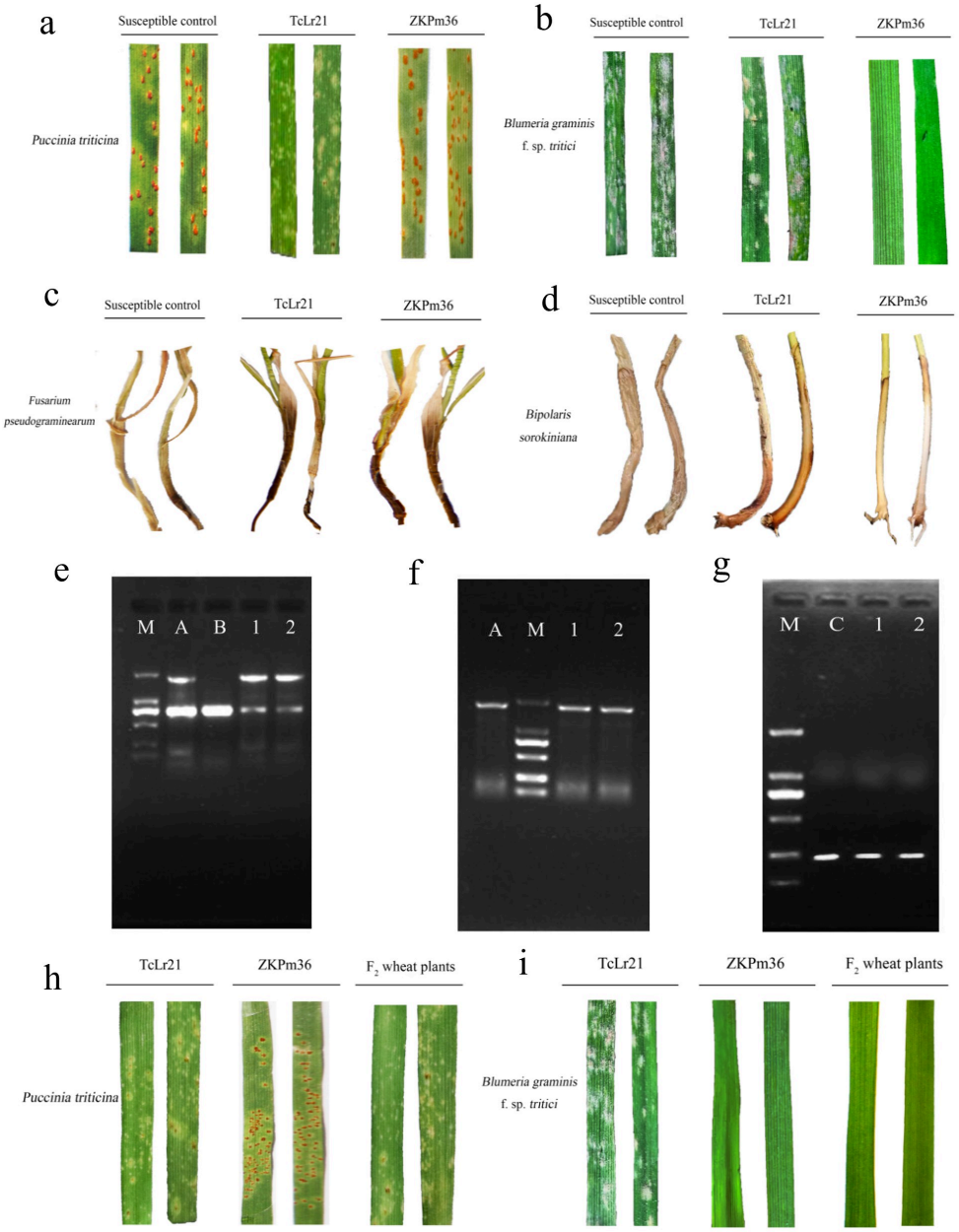


Fig. 6 Multi-disease resistance phenotyping and validation of parental lines TcLr21 and ZKPm36, their two hybrid progenies, and the F_2 generation

(a): Resistance to *Puccinia triticina* (leaf rust); **(b)**: *Blumeria graminis* f. sp. *tritici* (powdery mildew); **(c)**: *Fusarium pseudograminearum* (crown rot); **(d)**: *Bipolaris sorokiniana* (root rot) in TcLr21, Thatcher, and ZKPm36. **(e)**: Molecular detection of *Lr21*; **(f)**: *BstE* II digestion; **(g)**: Molecular detection of *Pm36* in F_1 hybrids. M: DNA marker; A: TcLr21; B: Thatcher; C: ZKPm36; 1-2: F_1 hybrids. **(h)** *Puccinia triticina* and **(i)** *Blumeria graminis* f. sp. *tritici*resistance in F_2 progenies. Representative results from three independent replicates are shown.

Figure 6

See image above for figure legend.

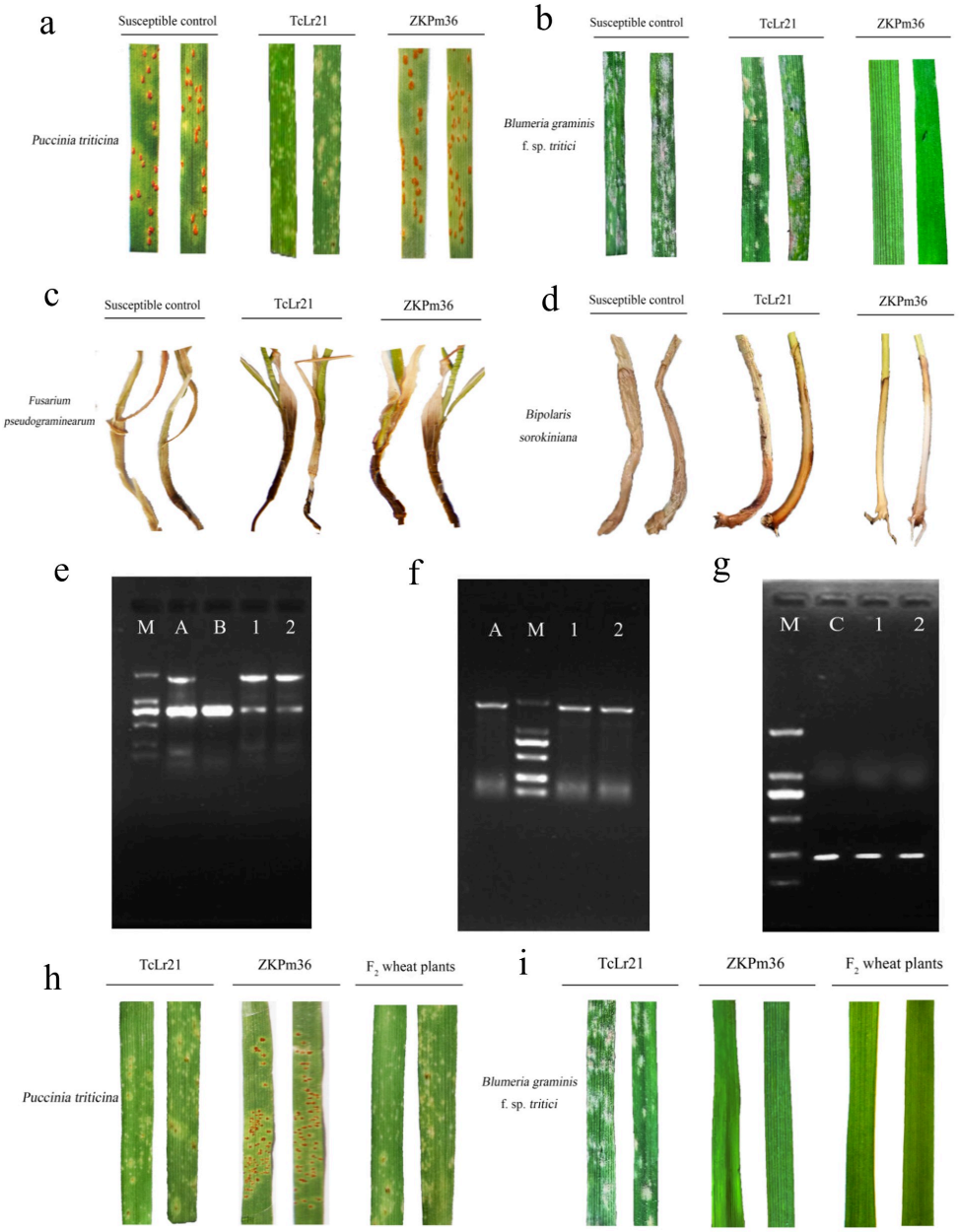


Fig. 6 Multi-disease resistance phenotyping and validation of parental lines TcLr21 and ZKPm36, their two hybrid progenies, and the F_2 generation

(a): Resistance to *Puccinia triticina* (leaf rust); **(b)**: *Blumeria graminis* f. sp. *tritici* (powdery mildew); **(c)**: *Fusarium pseudograminearum* (crown rot); **(d)**: *Bipolaris sorokiniana* (root rot) in TcLr21, Thatcher, and ZKPm36. **(e)**: Molecular detection of *Lr21*; **(f)**: *BstE* II digestion; **(g)**: Molecular detection of *Pm36* in F_1 hybrids. M: DNA marker; A: TcLr21; B: Thatcher; C: ZKPm36; 1-2: F_1 hybrids. **(h)** *Puccinia triticina* and **(i)** *Blumeria graminis* f. sp. *tritici*resistance in F_2 progenies. Representative results from three independent replicates are shown.

Figure 6

See image above for figure legend.

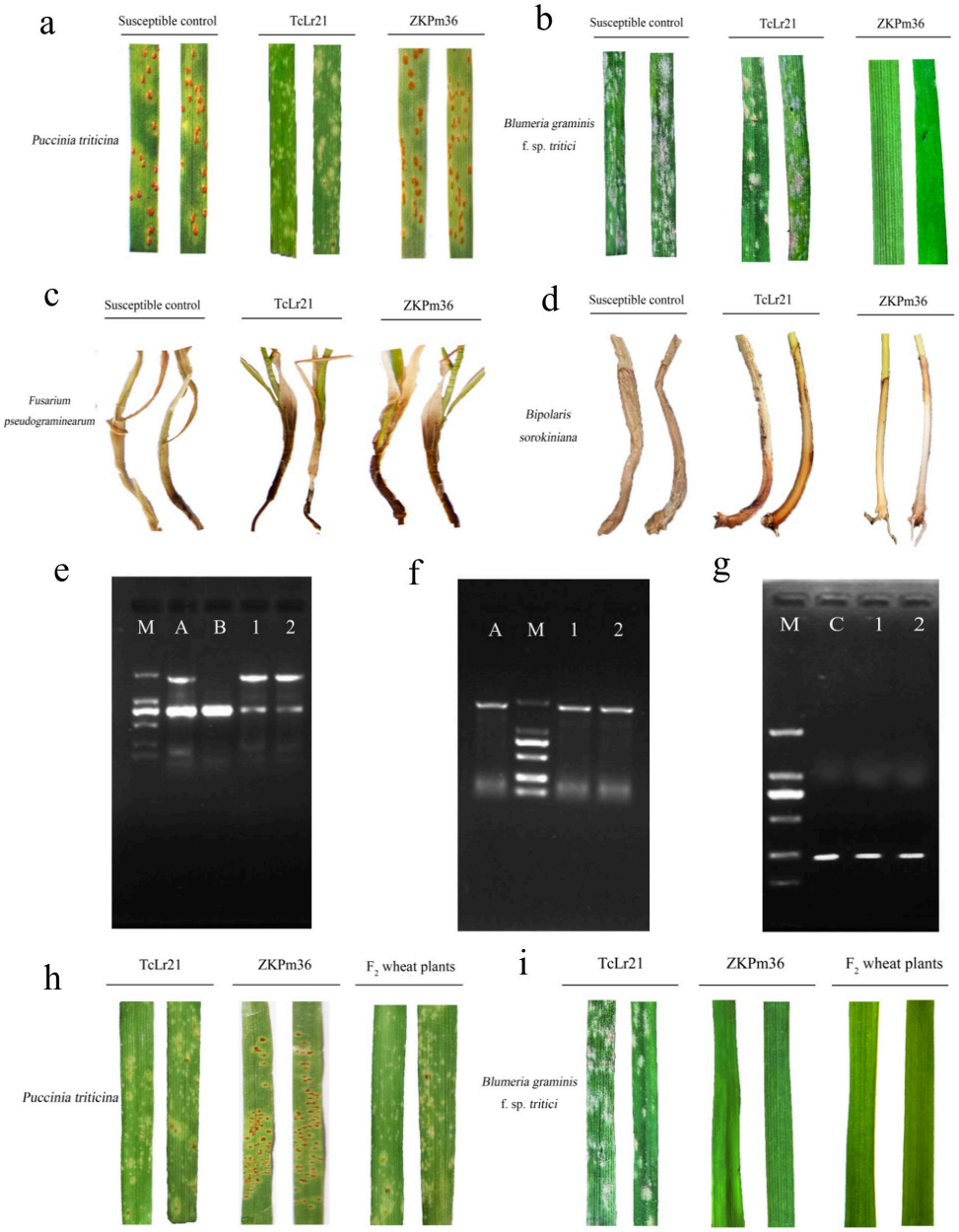


Fig. 6 Multi-disease resistance phenotyping and validation of parental lines TcLr21 and ZKPm36, their two hybrid progenies, and the F_2 generation

(a): Resistance to *Puccinia triticina* (leaf rust); **(b)**: *Blumeria graminis* f. sp. *tritici* (powdery mildew); **(c)**: *Fusarium pseudograminearum* (crown rot); **(d)**: *Bipolaris sorokiniana* (root rot) in TcLr21, Thatcher, and ZKPm36. **(e)**: Molecular detection of *Lr21*; **(f)**: *BstE* II digestion; **(g)**: Molecular detection of *Pm36* in F_1 hybrids. M: DNA marker; A: TcLr21; B: Thatcher; C: ZKPm36; 1-2: F_1 hybrids. **(h)** *Puccinia triticina* and **(i)** *Blumeria graminis* f. sp. *tritici*resistance in F_2 progenies. Representative results from three independent replicates are shown.

Figure 6

See image above for figure legend.

Supplementary Files

This is a list of supplementary files associated with this preprint. Click to download.

- SupplementaryFigures.docx
- SupplementaryFigures.docx
- SupplementaryFigures.docx
- SupplementaryFigures.docx
- SupplementaryTable.docx
- SupplementaryTable.docx
- SupplementaryTable.docx
- SupplementaryTable.docx
- SupplementaryFigureFulllengthgels.docx
- SupplementaryFigureFulllengthgels.docx
- SupplementaryFigureFulllengthgels.docx
- SupplementaryFigureFulllengthgels.docx